

ANNUAL  
PROGRESS REPORT

MASTER

Submitted to  
U. S. Energy Research and Development Administration

Submitted by  
Accelerator Laboratory  
Department of Physics  
Kansas State University  
Manhattan, Kansas 66506

NOTICE  
This report was prepared as an account of work sponsored by the United States Government. Neither the United States nor the United States Energy Research and Development Administration, nor any of their employees, nor any of their contractors, subcontractors, or their employees, makes any warranty, express or implied, or assumes any legal liability or responsibility for the accuracy, completeness or usefulness of any information, apparatus, product or process disclosed, or represents that its use would not infringe privately owned rights.

Reporting Period  
October 1, 1974 to September 30, 1975

Title: "ATOMIC AND NUCLEAR RESEARCH WITH ACCELERATORS"

Contract Number: E(11-1)-2130

Title: "FUSION RELATED ATOMIC PHYSICS"

Contract Number: E(11-1)-2753

October 1975

DISTRIBUTION OF THIS DOCUMENT IS UNLIMITED

EB

## DISCLAIMER

**This report was prepared as an account of work sponsored by an agency of the United States Government. Neither the United States Government nor any agency Thereof, nor any of their employees, makes any warranty, express or implied, or assumes any legal liability or responsibility for the accuracy, completeness, or usefulness of any information, apparatus, product, or process disclosed, or represents that its use would not infringe privately owned rights. Reference herein to any specific commercial product, process, or service by trade name, trademark, manufacturer, or otherwise does not necessarily constitute or imply its endorsement, recommendation, or favoring by the United States Government or any agency thereof. The views and opinions of authors expressed herein do not necessarily state or reflect those of the United States Government or any agency thereof.**

## **DISCLAIMER**

**Portions of this document may be illegible in electronic image products. Images are produced from the best available original document.**

## ABSTRACT

Atomic reaction mechanisms have been investigated by measuring x-ray and Auger production cross sections from high energy ion-atom collisions. Gas target results have been obtained for H, He, C, N, O and F beams on Ne; F, Cl and S beams on Ar and F on Kr as a function of the projectile charge state. K-shell x-ray production cross sections for H, C, N and O on thin solid targets of Ni, Rb, Ag and Sb have been measured. In addition L-shell and M-shell partial cross sections have been measured for H impact on several heavy elements. The impact parameter dependence of the probability for K x-ray production has been measured for O on Cu and for C and F on Ar as a function of projectile charge state. Electron capture to excited states of F projectiles in various gases has been investigated by measuring the K x-ray emission cross sections. The population of substates by electron capture processes has been studied by observations of the anisotropic angular distribution of this radiation. The relative multiple ionization fractions from ion-atom collisions and the resultant partial fluorescence yields have been deduced from high resolution emission spectra of Ne. The systematics of K x-ray satellite structure have been extended to Br beams on targets of Al, Sc and Ti. Lifetime measurements have been performed for the  $2^3S_1$  state of heliumlike S and Cl, the  $3^3P_1$  state of heliumlike S and the  $3d^9 4s-3d^{10}$  electric quadrupole transitions of  $I^{+25}$ . The radiative Auger effect and radiative electron rearrangement have been observed and identified in ion-atom collisions. Polarization of projectile x rays produced in thin C foils has been observed by measuring the in- and out-of-plane scattering from a Bragg crystal. Atomic theory calculations have been performed for the ionization cross sections of atoms by ions and electrons using the Glauber approximation. Theoretical x-ray spectra for ion-atom collisions have been predicted by combining structure calculations, fluorescence yields and configuration cross sections. Nuclear reaction mechanisms have been investigated through the study of (1) inelastic and elastic scattering of nuclei of He, C and N from various targets (2) resonances in the compound systems of  $^{12}\text{C}$  plus  $^{13}\text{C}$  and  $^{12}\text{C}$  plus  $^{15}\text{N}$ , (3) one- and two-neutron transfer reactions near the Coulomb barrier and (4) measurement of the lifetimes of low-lying levels of  $^{21}\text{Ne}$ . Materials study by x-ray fluorescence has been used to determine Br and Zn levels in untreated flour.

## TABLE OF CONTENTS

	Page
1. INTRODUCTION . . . . .	1
2. LABORATORY OPERATION AND DEVELOPMENT	
2.1 Tandem Van de Graaff Accelerator Operation and Improvements . . . . .	6
2.2 3 MV Van de Graaff Installation and Operation . . . . .	7
2.3 Sputter Ion Source Installation and Operation . . . . .	9
2.4 Auxiliary Equipment Improvements . . . . .	10
2.5 On-Line Computer System . . . . .	11
2.6 A Summary of Research Instruments Designed and Constructed in the Year Ending Sept. 30, 1975 . . . . .	11
2.7 Direct Extraction of a $C^-$ Beam from the Diode Ion Source . . . . .	14
3. ATOMIC COLLISION CROSS SECTIONS IN GASES	
3.1 K X-ray Production in Single Collisions of Chlorine and Sulfur Ions . . . . .	16
3.2 K X-ray Emission from 20- to 36-MeV Fluorine Projectiles Following Electron Capture to Excited States . . . . .	18
3.3 Argon and Krypton X-ray Production by Fluorine Projectiles of Different Charge States . . . . .	20
3.4 Ne K-Shell Auger Electron Cross Sections in .5 to 10.0 MeV $H^+$ -Ne Collisions . . . . .	21
3.5 Ne K-Shell Auger Cross Sections in 3- to 35-MeV $F^{+q}$ + Ne Collisions . . . . .	25
3.6 F-Ne K-Vacancy Sharing . . . . .	26
3.7 K-Shell Auger Electron Hypersatellites of Ne . . . . .	28
3.8 Argon K-Auger Cross Sections in Collisions with 30 MeV F Ions . . . . .	29
3.9 Neon K Fluorescence Yields for $N^{Q+}$ -Induced Collisions . . . . .	30

4.	IONIZATION CROSS SECTIONS IN THIN SOLID MATERIALS	
4.1	K-Shell X-Ray Production Cross Sections for $^{12}\text{C}$ , $^{14}\text{N}$ and $^{16}\text{O}$ in Thin Solid Targets . . . . .	31
4.2	High Resolution Studies of L-Shell Ioni- zation by Light Ions . . . . .	35
4.3	M-Subshell X-Ray Cross Section Measurements . . . . .	36
5.	EXPERIMENTAL IMPACT-PARAMETER DEPENDENT PROBABI- LITIES FOR K-SHELL VACANCY PRODUCTION BY FAST HEAVY-ION PROJECTILES . . . . .	37
6.	X-RAY SPECTROSCOPY WITH HIGH ENERGY IONS	
6.1	Radiative Auger Effect in Ion-Atom Collisions . . . . .	41
6.2	Radiative Electron Rearrangement: A Proposed Description for Low Energy Satellites Observed in Ion-Atom Collisions . . . . .	42
6.3	Enhancement of Radiative Electron Rearrange- ment in Si by $\text{He}^+$ Bombardment . . . . .	43
6.4	Multiplet Effects in High Resolution Ne $K\alpha$ Structure . . . . .	45
6.5	Charge-State Dependence of the Ne K Fluorescence Yield Deduced from High-Resolution Emission Spectra . . . . .	46
6.6	Relative Multiple Ionization Cross Sections of Neon by Projectiles in the 1-2 MeV/amu Energy Range . . . . .	47
6.7	$K\alpha$ Satellite X Rays in Al, Sc, and Ti Follow- ing Bromine-Ion Bombardment . . . . .	48
6.8	Neon $K\alpha$ , $K\beta$ Satellite Structure Induced by 80-MeV Argon-Ion Impact . . . . .	49
7.	ATOMIC LIFETIME MEASUREMENTS	
7.1	Lifetime Measurement of the $^3P_1$ State of Heliumlike Sulphur . . . . .	50
7.2	X Rays from Foil-Excited Iodine Beams . . . . .	50

	Page
7.3 Lifetime of the $2^3S_1$ State in Heliumlike Sulphur and Chlorine . . . . .	51
8. POLARIZATION STUDIES OF ION-INDUCED X RAYS	
8.1 Anisotropy of Characteristic K-Shell X Rays from Heavy-Ion-Atom Collisions . . . . .	55
8.2 Polarization Fractions of K X Rays Emitted by Fast Fluorine Ions Incident in Different Charge States on He . . . . .	55
8.3 Direct Measurement of the Linear Polarization of Lyman- $\alpha$ X Rays . . . . .	56
9. THEORETICAL SPECTRA IN ION-INDUCED REACTIONS	
9.1 Relative Multiple Ionization Cross Sections of Neon by Oxygen Ions . . . . .	58
9.2 Lifetimes and Fluorescence Yields of Three-Electron Ions . . . . .	62
9.3 Relativistic Contributions to Transition Energies in NiI and CuI Isoelectronic Sequences . . . . .	67
10. THEORETICAL ATOMIC CROSS SECTION CALCULATIONS	
10.1 K-Shell Ionization in Multielectron Atoms by Electron Impact Using the Single-Particle Glauber Approximation . . . . .	70
10.2 K-Shell Ionization Cross Sections by Proton Impact Using the Single-Particle Glauber Approximation . . . . .	72
10.3 Projectile Charge Dependence of Total Ionization Cross Sections in Atomic Hydrogen by Proton and Alpha Particle Impact . . . . .	74
10.4 Spectral Energy Distributions of Ejected Atomic Electrons . . . . .	76
10.5 Momentum Transfer Differential Cross Sections for Ionization . . . . .	76
10.6 Theoretical Definition of the Binomial Distribution of Single Electron Ionization and Excitation Probabilities . . . . .	77

10.7	Application of a Charge Paired Born Approximation to Charge Transfer . . . . .	78
10.8	Development of a Modified Eikonal Approximation for Charge Transfer . . . . .	79
10.9	DWBA Calculation of Excitation in Atoms and Ions by Charge Particles . . . . .	80
10.10	SCA Predictions of 2s-2p Transition Probabilities by Direct Coulomb Excitation . . . . .	81
10.11	Development of Born Code Including Coulomb Deflection and Binding Energy Corrections . . . . .	81
10.12	Role of Outer Shells in Born Cross Sections for K-Shell Ionization by Charged Particles . . . . .	82
11.	SEARCH FOR HEAVY-ION RESONANCES . . . . .	83
12.	LIFETIMES OF LOW-ENERGY STATES IN $^{21}\text{Ne}$ . . . . .	84
13.	NUCLEAR SCATTERING AND REACTIONS	
13.1	Analog Resonances and Possible $T_{\gamma}$ Mixing in $^{77}\text{Br}$ . . . . .	85
13.2	Systematics of Backward-Angle Elastic Alpha Scattering . . . . .	85
13.3	Optical-Model Analysis of N+C and C+C Elastic Scattering . . . . .	86
13.4	Comparison of One and Two-Neutron Transfer Near the Coulomb Barrier for the $^{27}\text{Al}(^{18}\text{O}, ^{16}\text{O})^{29}\text{Al}$ , $^{27}\text{Al}(^{18}\text{O}, ^{17}\text{O})^{28}\text{Al}$ and $^{27}\text{Al}(^{13}\text{C}, ^{12}\text{C})^{28}\text{Al}$ Reactions . . . . .	87
13.5	The Proton Optical-Model Potential Near the Coulomb Barrier . . . . .	87
13.6	Total Cross Sections for the $^{19}\text{F}(^{13}\text{C}, ^{12}\text{C})^{20}\text{F}$ and $^{23}\text{Na}(^{13}\text{C}, ^{12}\text{C})^{24}\text{Na}$ Reactions . . . . .	88
13.7	Energy Loss of Low-Energy $^{40}\text{Ca}$ Ions in Carbon . . . . .	88
14.	TRACE ELEMENT ANALYSIS	
14.1	The Determination by X-Ray Observation of Bromine and Zinc Levels in Untreated Wheat Flour . . . . .	90

	Page
14.2 Trace-Element Analysis by X-Ray Fluorescence with an External Proton Beam . . . . .	90
15. ATOMIC AND NUCLEAR PHYSICS LABORATORY PERSONNEL . . . . .	92
16. ADVANCED DEGREES AWARDED DURING 1974-75 ACADEMIC YEAR . . . . .	94
17. PUBLICATIONS FOR PERIOD 1 OCT 1974 - 30 SEPT 1975	
17.1 Published Papers Supported by ERDA Contract E(11-1)-2130 . . . . .	95
17.2 Papers Submitted for Publication and Supported by ERDA Contract E(11-1)-2130 . . . . .	98
17.3 Papers Submitted for Publication and Supported by ERDA Contract E(11-1)-2753 . . . . .	99
17.4 Abstracts of Contributed Papers . . . . .	100
17.5 Invited Talks Presented by Staff . . . . .	102
17.6 Review Papers for Textbook Publication . . . . .	103
18. ACKNOWLEDGMENT OF SUPPORT . . . . .	104

## 1. INTRODUCTION

This progress report includes a summary of the research performed by the Kansas State University atomic and nuclear physics group (listed in section 15 of this report) for the period October 1, 1974 to September 30, 1975. The major effort for this period has once again been in the area of basic atomic physics involving high-energy, few-electron ions. The two main categories of our atomic research are reaction mechanism studies and spectroscopy of ion-atom collisions. Measurements of various reaction cross sections for ions in tenuous gases and thin solids, atomic lifetimes of metastable ions, x-ray and Auger spectroscopy in ion-atom collisions, and polarization of atomic radiation from ion-atom collisions have been performed and the results presented herein. The theoretical work, which consists of atomic cross section calculations for e-atom and ion-atom collisions, and calculation of theoretical spectra of ion-induced reactions, is included in our progress report for the first time. A strong coupling between the theoretical and experimental programs has been realized this year through the inclusion of the theory in the accelerator program. We anticipate that these collaborative efforts will significantly strengthen the overall effectiveness of our near and long range contributions to atomic physics.

The atomic physics group has become more aware in the past year of the need, by other areas of physics, such as high temperature plasmas (HTP), for high energy high Z reaction data and calculations we are capable of providing. Examples of work related to other areas are (a) the calculation of lifetimes and fluorescence yields of three-electron ions

required in the analysis of electron number density and temperatures of plasmas, (b) the measurement of the spectra and lifetimes of highly ionized iodine which extends the results of laser-induced plasma studies, (c) the calculation of transition energies for  $3d^9 4s \rightarrow 3d^{10}$  electric quadrupole and the  $3d^9 4p \rightarrow 3d^{10}$  electric dipole decays in the NiI and CuI isoelectronic sequences, and (d) the measurement of large x-ray cross sections in hydrogen and helium following electron capture to excited states. These efforts have become an integral part of the laboratory program since the funding of a new ERDA contract entitled "Fusion Related Atomic Physics" in June 1, 1975. An expanded program in this area is anticipated for next year. In particular, a series of experiments on crossed ion-electron beams will be designed, constructed and performed.

The atomic physics program has been greatly enhanced through our visiting faculty program which is supported by Kansas State University. During the last year we have had four visitors in the persons of Prof. T. J. Gray from North Texas State University in Denton; Dr. E. N. Pedersen from the University of Aarhus in Aarhus, Denmark; Prof. E. Salzborn from the University of Giessen in Giessen, W. Germany; and Dr. N. Stolterfoht of the Hahn-Meitner Institute in Berlin, W. Germany. Professor Gray will be at Kansas State through the summer of 1976. We will have in addition the good fortune of having Professor Teijo Åberg from the Technical Institute of Finland in Helsinki join our staff as a visitor in January 1976.

As in past years, a program of heavy-ion nuclear physics research has been continued and several interesting results have been obtained. Some results on the measurement and analysis of heavy-ion

elastic scattering (e.g. C + C and N + C) and heavy-ion compound nucleus resonances (e.g.  $^{12}\text{C} + ^{13}\text{C}$  and  $^{12}\text{C} + ^{15}\text{N}$ ) are presented. Nuclear lifetime measurements in  $^{21}\text{Ne}$  have been measured by Doppler-shift attenuation in the  $^{12}\text{C}(^{13}\text{C},\alpha)^{21}\text{Ne}$  reaction and lend support to a Nilsson model description for the low-lying levels.

Another area of laboratory interest is in applied physics. In addition to the atomic collision studies applied to HTP, as mentioned above, material studies are being performed by the x-ray fluorescence technique. Also, a feasibility study is being made to assess the possibility of using the Mössbauer effect to obtain real time information on radiation damage in solid materials.

The laboratory program is centered about the 6 MV tandem accelerator and auxiliary equipment as depicted in the first figure. A PDP-15 computer with a background/foreground monitor system is used in on-line data accumulation and off-line data analysis. A new heavy-ion sputter source has been added to the tandem during the last year. In addition a 3 MV single-ended Van de Graaff has been installed and used in several experiments. The operation and developments in the laboratory facilities are discussed in section 2.

The research output of the laboratory in the last year can best be summarized by noting the following: (a) 27 papers were published under Contract E(11-1)-2130 and an additional 10 papers are at the preprint stage; (b) 11 additional papers are in the preprint stage for the new contract E(11-1)-2753; (c) 19 contributed papers and 9 invited talks were presented at American Physical Society and international conferences;

(d) 4 review papers written for textbook publication, and (e) 5 Ph.D. degrees were granted from laboratory research efforts. Our Ph.D. students have been sought by many laboratories in the U. S. and abroad. The latest five Ph.D. graduates have accepted jobs at Bell Laboratories, Los Alamos Scientific Laboratory, Fusion Energy Corporation, Dresser Industries, and East Carolina University.

ACCELERATOR LABORATORY  
KANSAS STATE UNIVERSITY  
DEPARTMENT OF PHYSICS  
FLOOR PLAN

5

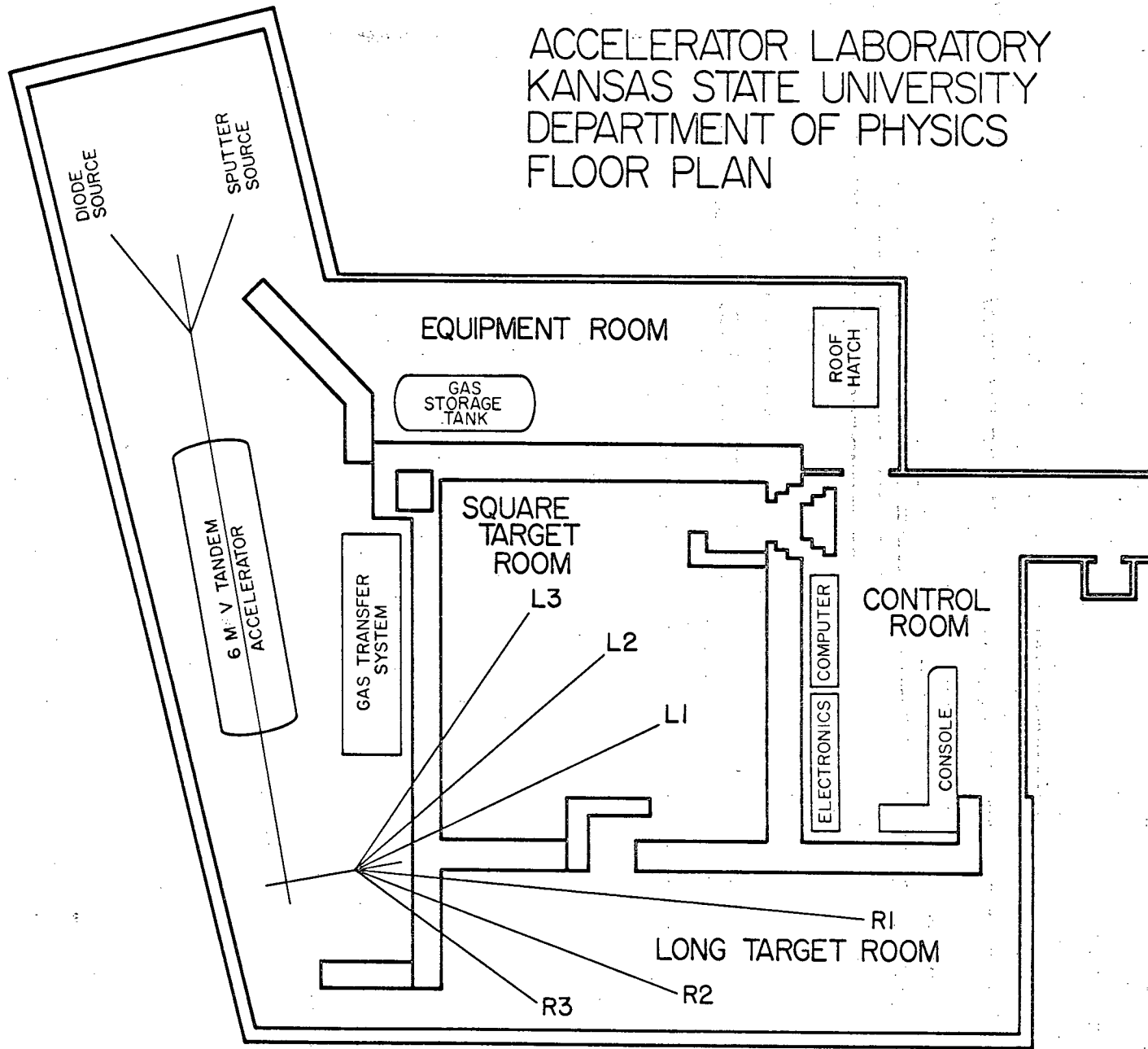


Fig. 1  
Sec. 1

## 2. LABORATORY OPERATION AND DEVELOPMENT

### 2.1 Tandem Van de Graaff Accelerator Operation and Improvements

During the period from October 1, 1974 to September 30, 1975, there were two major installations to the 6 MV tandem Van de Graaff accelerator at Kansas State University.

First was the removal of the old charging belt and the installation of a new charging belt which was purchased from High Voltage Engineering Corporation, Burlington, Massachusetts. The old belt was put in service June 22, 1972, and when removed had a total of 12,990 hours of service. The reason for the change was that the total service hours exceeded the recommended lifetime which is 10,000 hours. After inspection of the old belt it was decided that it could be kept as a spare and at present serves as the only spare.

The second major installation was the removal of the old high energy straight tubes and the installation of the new inclined field tubes purchased from High Voltage Engineering Corporation. The removed straight tubes were the original tubes that came with the tandem and had 23,376 hours of service. These tubes were removed because they did not allow the tandem to hold voltage reliably above 5 MV on the terminal due to radiation damage and surface contamination. The new inclined field tubes were brought into optical alignment with the external beam transport according to specifications recommended by High Voltage Engineering Corporation. This was engineered by R. Krause, E. J. Feldl, and M. D. Wells.

To this date the tandem has been operating at its recommended voltage of 6 MV with 2,502 hours on the new belt and 2,371 hours on the

new tubes. The only problem encountered since the major installations has been accumulation of belt dust caused by conditioning of the new belt. This has caused dust bridges to develop across the belt spacers causing a vertical instability in low-energy beams. This problem can be corrected by periodic maintenance on the high energy column of the tandem. Once the charging belt is sufficiently conditioned, we should no longer have the dust-bridging problem.

The total down time during the reporting period was 1290 hours. Of this time, over half (744 hours) was for the major installations discussed above. The remaining 546 hours was for periodic maintenance of such items as collector screens, stripper foils, broken resistors, etc.

(R. Krause)

## 2.2 3 MV Van de Graaff Installation and Operation

A modified AK-N High Voltage Engineering Corporation Van de Graaff accelerator has been added to the research facilities at Kansas State University. The accelerator was purchased from Texas Nuclear Corporation, Austin, Texas and disassembled and transported by Professor Richard and four of his graduate students. The funds for the purchase and transportation were made available by the university. After reassembly and initial testing, several improvements were made.

- 1) A source thermo-mechanical leak was installed to give the machine heavy-ion capability in addition to its proton and deuteron beam capabilities.

- 2) A new set of column resistors was installed to make the machine operation more stable.
- 3) Three beam lines have been set up with diffusion pump vacuum systems.
- 4) Electrostatic quadrupoles were added for more efficient beam focussing, and
- 5) The analyzing magnet has been calibrated with a solid-state Hall probe.

The machine has been in operation 400 hours in testing and experimental work. At the present time it is capable of accelerating  $H^+$  and  $He^+$  in an energy range from 0.4 to 2.2 MeV. This extends the existing range of beams and energies available from the tandem Van de Graaff and should be of great use to the accelerator research program.

(K. A. Jamison)

### 2.3 Sputter Ion Source Installation and Operation

The universal negative ion source (UNIS source) purchased from Extrion Corporation in August of last year is being used with limited success. This UNIS source is a Mark VI version of the sputtering type negative ion source that produces a negative ion beam by the sputtering of material from a target cone bombarded by a high current primary beam of cesium positive ions. This process produces several  $\mu$ amp quantities of negative ion beams over a large range of atomic Z. A partial list of beams that can be obtained is H, D, Li, B, S, C, O, Ti, Cu, Ni, Be, Al, Cl, Br, Pb, Mg and U. Our source is presently installed with solid cones of Li, Be, C, Al, Ti, Fe, Cu and Pb. Beams of a few microamps have been obtained at the source for several elements; however, initially the transmitted beam through the tandem has been only a few percent at best. Recent attempts have increased the transmission to  $\sim 10\%$ . Additional problems such as vacuum failure of the cesium boiler, line voltage drop in power to the source and power supply failure due to sparking have hampered considerably the effective use of the source.

The source has been carefully realigned with the tandem in order to obtain the significant improvement in beam transmission. Further improvements in transmission are expected to be dependent on improved optics of the cesium ion transport. A radiation hazard initially present at the vicinity of the source has been reduced substantially by deflecting electrons in the source prior to acceleration.

Improved operation of the source is being sought continually.

(J. R. Macdonald)

## 2.4 Auxiliary Equipment Improvements

Several improvements have been made and are in the process of being made with the auxiliary equipment in the laboratory. During the month of May, we replaced an E-MAG-32 High Voltage Engineering Corporation quadrupole on L-1 beamline, due to bad coils, with a new High Voltage Engineering Corporation quadrupole C-MAG-516 at a cost of \$2,300. The quadrupoles on L-1 and L-2 beamlines are similar and thus use the same power supply; whereas, the L-3 quadrupole is still being used with the old model 400V-2A HVEC power supply. Beam lines are labeled in the figure in section 1.

October installations include three new power supplies. One HVEC, Model 2400-301, 12 kW, 300 amp supply at a cost of \$10,100 and two electronic measurements SCR 300V-1.5A supplies at a cost of \$475 each.

The model 2400-301 solid state supply will replace an old solid state plus tube type HVEC D-PS-34 power supply currently being used on the switching magnet. This supply is old and very unstable.

The two solid state electronic measurement supplies Models SCR 300V-1.5A will be used in place of the very old power supply Model 400V-2A built by HVEC. The supplies are being used to power quadrupoles on beamlines R-1 and R-2.

(R. Krause and M. Wells)

## 2.5 On-Line Computer System

A Canberra model 8100 analog-to-digital converter system was interfaced to the PDP-15 computer to allow an additional data acquisition mode. This has been especially useful for multiple detector experiments. Further, the display terminal in the background portion of the computer has been optimized for faster plotting.

Software development includes changes in data acquisition programs to handle the Canberra system, the capability of making a line printer plot of data from both foreground and background terminals, and adaptation of the latest monitor system from DEC for local use.

(G. G. Seaman)

## 2.6 A Summary of Research Instruments Designed and Constructed in the Year Ending September 30, 1975. Minor Projects and Modifications to Existing Apparatus are not Included.

1) Performance description and characteristics of an electron spectrometer that was designed and constructed are mentioned elsewhere in this report. The physical overall dimensions of this instrument are 10 inches diameter by 24 inches long. Electron deflection envelope diameter is 6.743 inches with a slit to slit distance of 6.324 inches, on a 3.220-inch diameter inner cylinder. Provisions were made for solid and gaseous targets, fine tuning of electron multiplier position, measurements of forward as well as back angle of beam products, cylindrical double magnetic shielding, convenient

alignment to beam, adjusting slit openings and an operating pressure in the  $10^{-6}$  Torr range.

Two support stands with the necessary alignment adjustments facilitate using this electron spectrometer in our 69-inch as well as our 42.5-inch (beam height) laboratory configurations.

2) An ARL 4-inch curved crystal Bragg spectrometer with flow-mode proportional counter was incorporated into a system which includes a target chamber, beam collimation, remote spectrometer drive and a support system which allows angular adjustment of the spectrometer to beam relationship for out-of-plane measurements.

The spectrometer was modified in several ways to obtain vacuum integrity, increase pump-out speed, allow for target chamber connection and rotation and to relocate the entrance slit.

The target diameter was designed to incorporate the rotatable vacuum seal, a Faraday cup with electron suppression, beam collimation, fixed monitoring detector locations, a multiple foil target wheel and a gas cell which allows the use of a gaseous target without having to remove the target wheel.

A support system, designed to operate at both the 69-inch and 42.5-inch beam locations, incorporates "T" slot type circular mounting tracks and angular position readout. It also locates and supports vacuum pumps.

3) To trap residual gas, upstream of an ongoing experiment, an in-line cold trap was designed and mounted to a beam line. The tubular trap is 12 inches long and 1.5 inches in diameter, is mounted to a 4-inch

beam line "T" and attached to an 8 hour LN<sub>2</sub> reservoir.

4) A velocity drive system for Mössbauer effect studies, with a vibration free mounting base and optical bench type component adjustment was designed and constructed.

5) A target chamber for charged particle induced x-ray fluorescence studies. The chamber dimensions are 4x4x4 inches, with six ports for beam entry, beam exit, ladder type target mount, viewing window, pumping port and detector port incorporating an optional and thin mylar window.

6) A new lid assembly for a previously designed Bragg detector target chamber includes a very precise linear track. External micrometer adjustable motions are transferred through vacuum seals to the inside of the target chamber where position and adjustments must be known to within  $\pm 0.002$  inches.

7) A foil stripper, used between the analyzing magnet and switching magnet of our 12 MeV tandem Van de Graaff accelerator, was designed. It has a ladder type foil mount with external foil selection, a viewing section to inspect foils and an air-lock to allow changing of foils without letting the beam line up to atmospheric pressure.

A slim line 1.5 inch gate valve was designed for this air lock. It is a split body, wedge type valve made of aluminum with a Delrin A.F. gate. Bolted connections on the gate valve are also compatible with the standard 2-inch dependex fittings we use in the accelerator laboratory to allow the use of this particular valve design in other applications.

8) An addition to one of our accelerator experiment stations was an ion implantation assembly. A crystalline target can be adjusted

externally in respect to the ion beam in two directions in addition to angular adjustments of the mounting platform. Adjustable beam collimation and a Faraday cup with electron suppression are incorporated.

(Eric Feldl)

## 2.7 Direct Extraction of a $C^-$ Beam from the Diode Ion Source.

The standard technique for production of C beams with the direct-extraction diode ion source involves introducing a mixture of methane and nitrogen gas into an intense hydrogen arc. The  $CN^-$  ion can then be extracted and produces a high intensity beam (1-3  $\mu A$ ) for injection into a tandem Van de Graaff accelerator. For achieving high energy C beams the  $CN^-$  beam suffers from the fact that the stripping at the terminal of the Van de Graaff yields only low intensity beams of the high charge states of C. This arises because of the low velocity of the  $CN^-$  ion at the stripping foil. To overcome this difficulty it is desirable to extract directly a  $C^-$  beam from the ion source.

Production of  $C^-$  ions from hydrocarbons has been unsuccessful with the diode source. In particular, we have only been able to obtain 10-30 nA of  $C^-$  beam from the diode ion source using a mixture of methane and nitrogen.

Introduction of carbon-monoxide gas into the intense hydrogen arc, however, has consistently yielded beams of  $C^-$  ions of reasonable intensity (450-600 nA) from the diode source. Although this is a factor

of 2-5 less than that which can be obtained from the source with  $CN^-$  beams the yield of the accelerated  $C(4+)$  beam is approximately the same as with  $CN^-$  and the yield of  $C(5+)$  is about a factor of 2-3 higher with  $C^-$  ions than with  $CN^-$ .

The  $C^-$  beam produced by this method has been useful for obtaining high energy  $^{12}C(5+)$  beams for utilization in nuclear physics experiments at KSU. It should be pointed out that the less intense  $C^-$  beam introduced into the Van de Graaff accelerator produces less electron and radiation loading of the generator and therefore more stable running conditions.

(J. S. Eck and D. O. Elliott)

### 3. ATOMIC COLLISION CROSS SECTIONS IN GASES

#### 3.1 K X-Ray Production in Single Collisions of Chlorine and Sulfur Ions

X-ray-production cross sections of both target and projectile were measured in collisions of 3.0 - 52.2-MeV Cl ions with a variety of thin, gas targets from He to Xe. The dependence of these cross sections on incident projectile charge state was measured for both Cl and S projectiles at one velocity ( $10^9$  cm/sec). The dependence of the projectile K x-ray-production cross sections on target atomic number  $Z_2$  is nonmonotonic, anomalously large cross sections being observed in the region of nearly symmetric collisions ( $Z_2 \sim 17$ ). For Cl-on-Ar collisions, the Cl K x-ray cross sections exhibit a weaker dependence on projectile energy than for asymmetric collisions such as Cl on Kr; hence, the dependence of the Cl K cross sections on  $Z_2$  approaches (and eventually reaches) monotonicity with increasing projectile energy. These observations indicate that the dominant K-vacancy-production processes at these projectile velocities (0.1-1.5 MeV/amu) are different for quasisymmetric collisions than for asymmetric collisions. Processes associated with the formation of a transient molecule may be largely responsible for K-vacancy production for the former.

The incident-charge-state dependence of x-ray-production cross sections also points to differences between symmetric and asymmetric collisions. This dependence is significantly greater for the former than for the latter in nearly all cases. (An exception is the Ne K cross section which increases very rapidly with charge state, as a result of the increasing Ne K fluorescence yield). The enhanced charge-state

dependence of x-ray cross sections for the nearly symmetric collisions suggests the increasing importance of  $2p\pi-2p\sigma$  transitions in K-vacancy production as the number of initial projectile 2p vacancies increases. For Cl projectiles with no initial 2p vacancies, however, the energy dependence of total K-vacancy-production cross sections in Cl-on-Ar collisions is much stronger than theoretical results for the  $2p\sigma-2p\pi$  cross section. For such cases, a different K-vacancy-production mechanism may be dominant; Meyerhof<sup>1</sup> has suggested that this mechanism is the excitation of  $2p\sigma$  electrons, to high n, or continuum states.

For the collision partner of higher atomic number in the nearly symmetric collisions, the transitions in the preceding discussion cannot directly contribute to K-vacancy-production. However, the cross sections for the higher-Z partner are observed to be very similar to the lower-Z partner in magnitude and charge-state dependence. Meyerhof<sup>2</sup> has proposed that a K-vacancy transfer mechanism may explain such similarities. This process is generally referred to as K-vacancy sharing. Comparison of the data with calculation of the probability for transfer of a K vacancy from the lower-<sup>13</sup>/<sub>3</sub> to the higher-Z collision partner indicate that this mechanism may indeed be operative in the collisions studied.

1) W. E. Meyerhof, Phys. Rev. A 10, 1005 (1974).

2) W. E. Meyerhof, Phys. Rev. Lett. 31, 1341 (1973).

(Loren Winters, Matt D. Brown, Louis D. Ellsworth, Tang Chiao, E. W. Pettus,  
and James R. Macdonald)

### 3.2 K X-Ray Emission from 20- to 36-MeV Fluorine Projectiles Following Electron Capture to Excited States

The projectile K x-ray emission cross sections for fluorine ions were measured under single collision conditions for charge states ranging from +4 to +9 in a thin argon target. The dependence of these cross sections upon the energy and the initial charge state of the projectile was determined for fluorine ions with energies between 20 and 36 MeV. Over the entire energy range, the K x-ray-production cross section for  $F^{+9}$  ions was about 70% of the total electron-capture cross section determined in a separate experiment. The K x-ray production cross section for these fully stripped ions is attributed to electron capture to excited states of the projectile.

For the bare ( $F^{+9}$ ) projectile, the K x rays observed are radiative decays which only occur following electron capture to excited states of the projectile; while in the more complicated case for the one-electron ( $F^{+8}$ ) beam, this electron capture dominates excitation processes in the production of K x rays. The experimental  $F^{+8}$  and  $F^{+9}$  x-ray-production cross sections are compared to predictions for electron capture calculated in a Brinkman-Kramers<sup>1</sup> approximation. For this comparison the calculations were normalized to the total experimental electron-capture cross sections.<sup>2</sup> Excellent agreement was found between both the  $F^{+9}$  and  $F^{+8}$  x-ray-production cross sections and the predicted cross section for capture to excited states. From the experiment with the bare nucleus, the K x-ray production is about 70% of the total capture cross section while for the calculated

results excited-state capture is about 90% of the total.

1) H. C. Brinkman and H. A. Kramers, Proc. Acad. Sci. Amsterdam 33, 973 (1930).

2) S. M. Ferguson, J. R. Macdonald, T. Chiao, L. D. Ellsworth, and S. A. Savoy, Phys. Rev. A 8, 2417 (1973) and T. Chiao, Ph.D. thesis (Kansas State University, 1973) (unpublished).

(M. D. Brown, L. D. Ellsworth, J. A. Guffey, T. Chiao, E. W. Pettus, L. M. Winters, and J. R. Macdonald)

### 3.3 Argon and Krypton X-Ray Production by Fluorine Projectiles of Different Charge States

In this work we measure Kr K and Kr L x-ray yields produced by incident 36- and 48-MeV F ions with charge states from +6 to +9. Additional data have also been acquired for Ar K x-ray yields obtained with 36- and 48-MeV F ions. As the  $Z_1/Z_2$  ratio is decreased from  $\frac{1}{2}(F^{q+}$  on Ar) to  $\frac{1}{4}(F^{q+}$  on Kr), we observe a significant decrease in the dependence of the target x-ray yield on the projectile charge state. In addition, although the direct Coulomb-ionization theory<sup>1,2</sup> does not correctly predict the absolute magnitudes of the cross sections for the fully stripped ions, we note that the observed projectile energy dependence of these cross sections is in general agreement with the theoretical predictions. When corrections for increased binding and Coulomb deflection are applied to the data as described by Basbas et al.,<sup>3</sup> the Ar data shows a larger disagreement with theory than without the corrections. For the Kr case, the measured cross section is larger than theory with the latter two corrections and smaller than theory by the same amount without the corrections. It has been indicated<sup>3</sup> that discrepancies of this type may be due to polarization of the K-shell orbit. Since the details of this effect have not yet been published, no polarization corrections are included.

1) E. Merzbacher and H. W. Lewis, in Handbuch der Physik, edited by S. Flügge (Springer-Verlag, Berlin, 1958), Vol. 34, p. 166ff.

2) J. D. Garcia, Phys. Rev. A 1, 280 (1970); 4, 955 (1971); J. D. Garcia, R. J. Fortner, and T. M. Kavanagh, Rev. Mod. Phys. 45, 111 (1973).

(Stephen J. Czuchlewski, James R. Macdonald, and Louis D. Ellsworth)

### 3.4 Ne K-Shell Auger Electron Cross Sections in .5 to 10.0 MeV $H^+$ -Ne Collisions

The cross sections for Ne K-shell Auger electrons have been measured for  $H^+$  projectiles from .5 to 10 MeV. These measurements were performed with a cylindrical mirror analyzer designed and built at Kansas State University. Fig. 1 shows the dimensions and the geometry of the analyzer. The line labeled as B denotes the beam axis for the "backward" mode. With this geometry electrons from  $90^\circ$  to  $174^\circ$  with respect to the beam axis are analyzed by electrostatic focussing of a  $42^\circ$  acceptance cone of the ejected electrons into a continuous channel electron multiplier. Typical resolution obtained from this system was 1.5% and peak-to-background ratios were typically 40 to 1 for  $H^+$  induced spectra.

Fig. 2 shows the Ne K-shell Auger cross section as a function of energy. Since the fluorescence yield is small for the states populated by  $H^+$  bombardment and charge exchange and molecular effects are expected to be small, we can compare the Auger production cross sections directly to the Coulomb ionization predictions based on various approximations. The predictions of the binary encounter approximation (BEA),<sup>1</sup> plane wave Born approximation (PWBA),<sup>2</sup> and a recent Glauber approximation<sup>3</sup> are plotted for comparison. Although all three theories show reasonable agreement, the quantum mechanical theories seem to better predict the shape of the energy dependence from 2.0 to 10 MeV.

<sup>1</sup>J. H. McGuire and P. Richard, Phys. Rev. A 8, 1374 (1973).

<sup>2</sup>G. S. Khandelwal, B.-H. Choi, and E. Merzbacher, Atomic Data 1, 103  
(1973).

<sup>3</sup>J. E. Golden, Ph.D. thesis (Kansas State University, 1975).

(C. W. Woods, R. L. Kauffman, K. A. Jamison, and P. Richard)

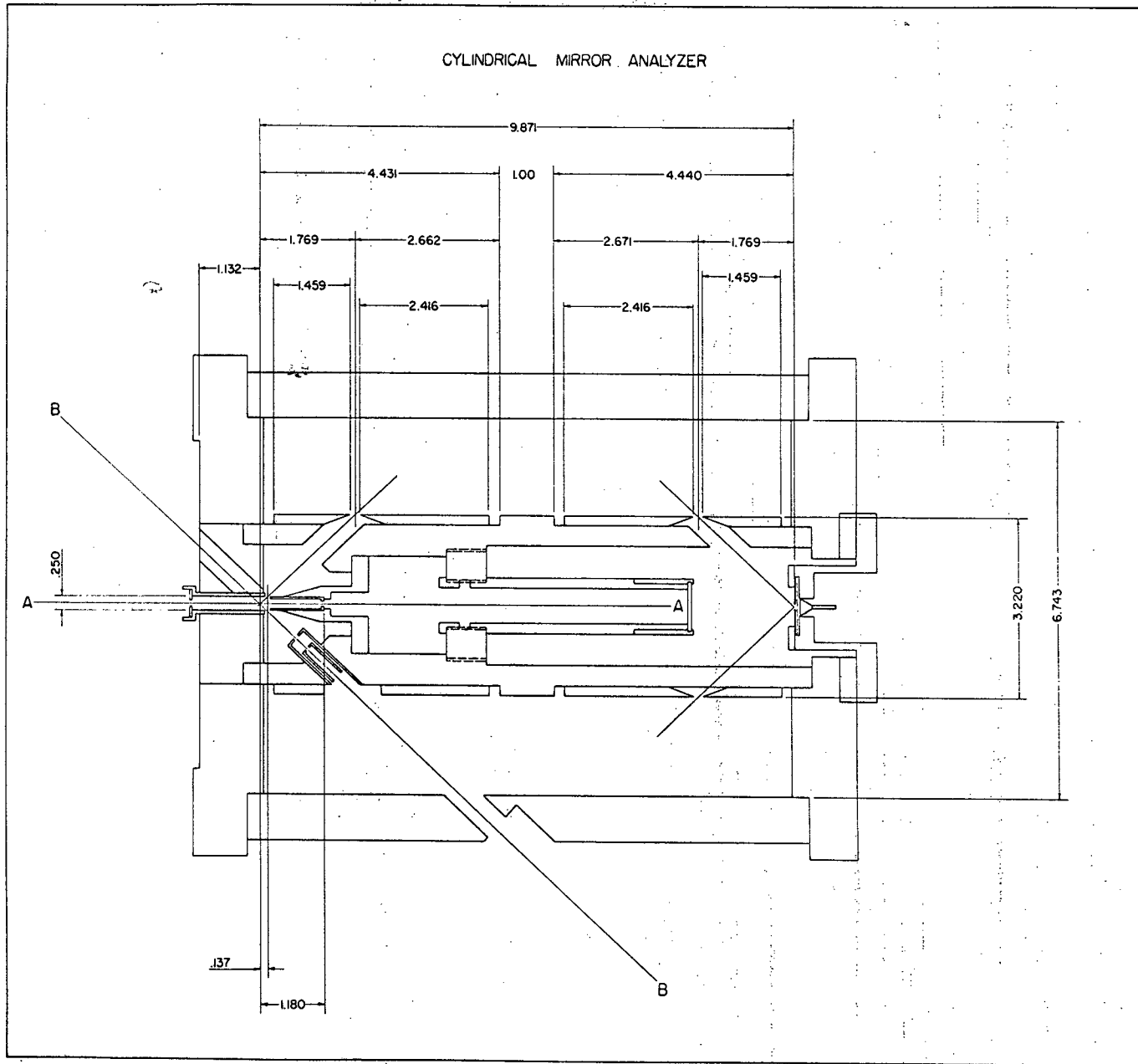


Fig. 1  
Sec. 3.4

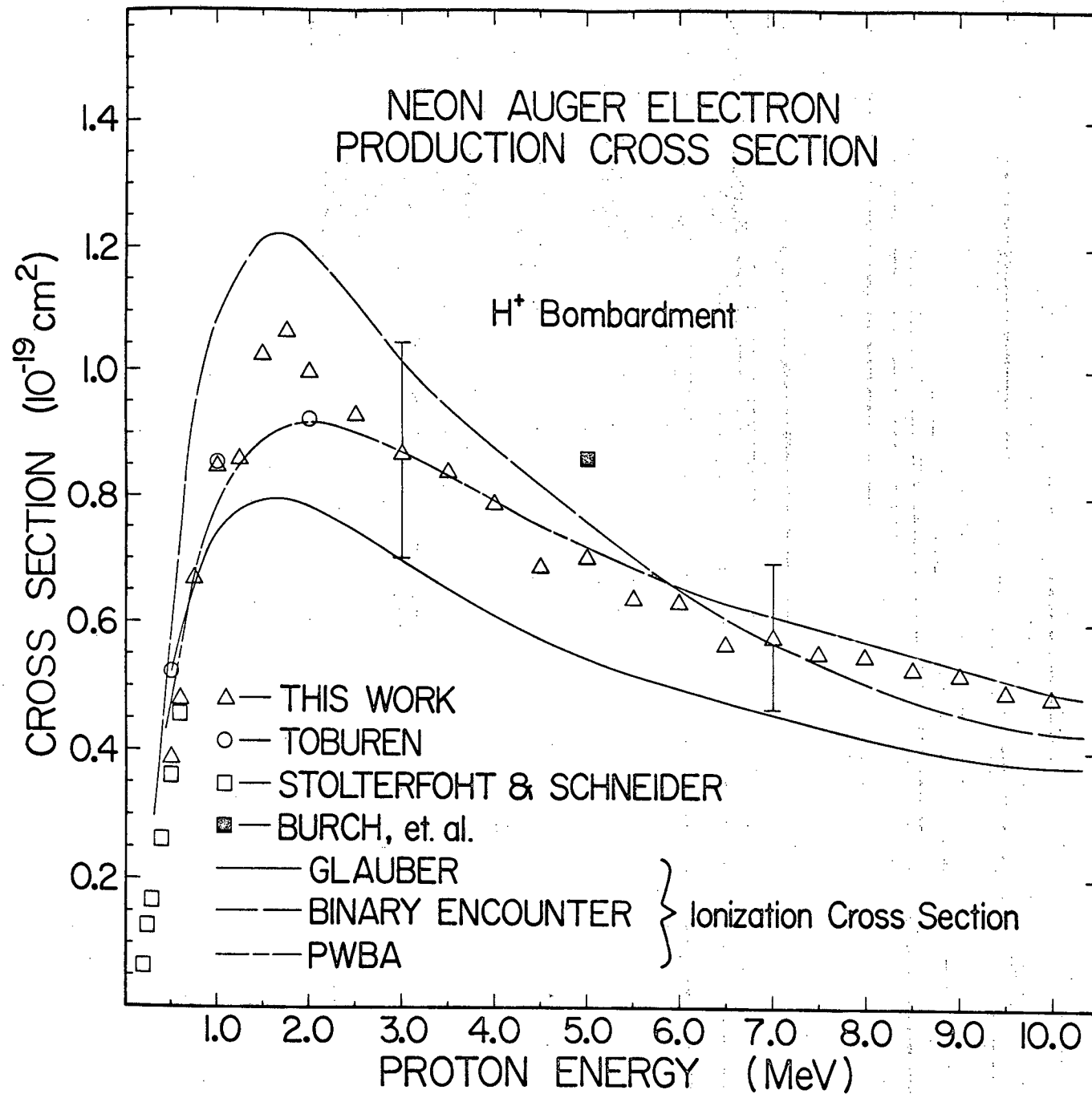


Fig. 2  
Sec. 3.4

### 3.5 Ne K-Shell Auger Cross Sections in 3- to 35-MeV $F^{+q}$ + Ne Collisions

The energy dependence of Ne K-shell Auger electron cross section has been measured for various charge states of F ions from 3- to 35-MeV. These measurements span the intermediate energy region for K-shell vacancy production from low energy collisions where the molecular promotion model is an effective theory to the high energy region where Coulomb ionization dominates. The experiment consisted of various energy F ions having charge states of +3 to +9 bombarding Ne gas in the cylindrical mirror electron analyzer described above.

At energies higher than 15 MeV the shape of the Auger cross sections follows closely the shape predicted by Coulomb ionization and the magnitude agrees with the  $F^{+8}$  data. Between 3 and 15 MeV the  $F^{3+}$  induced cross sections differ from the Coulomb ionization prediction by as much as a factor of 5.  $Ne^+$  on Ne data from 50 keV to 2.2 MeV can be qualitatively understood by the molecular promotion (MO) process which suggests that the region between 3 and 15 MeV must include both Coulomb and MO processes.

The only other study of K-shell vacancy productions at intermediate energies is for symmetric Al-Al and Ni-Ni collisions<sup>1</sup> using thin solid targets. Because of the charge state distribution in the solid target, these data do not contain the explicit charge state dependence presented in this study.

<sup>1</sup>) R. Laubert, H. Haselton, J. R. Mowat, R. S. Peterson, and I. A. Sellin, Phys. Rev. A (to be published).

(C. W. Woods, R. L. Kauffman, K. A. Jamison, N. Stolterfoht, and P. Richard)

### 3.6 F-Ne K-Vacancy Sharing

To test the assertion that molecular orbital (MO) processes are affecting the Ne K-shell Auger electron cross sections for F bombardment below 15 MeV, the F K-shell projectile Auger electron production cross sections were measured for bombarding energies of 3 to 15 MeV. For kinematical reasons these measurements were performed with the cylindrical electron analyzer in the forward mode so that only electrons emitted at  $42^\circ$  from the beam axis were analyzed.

Fig. 1 shows the ratio of the Ne to F Auger electron production cross section as function of the F velocity. The Ne cross sections were measured in the backward mode except at energies below 5 MeV where it was possible to extract both the F and Ne cross sections from a single spectrum. Kinematically corrected yields were used to calculate the ratio R shown in Fig. 1. The vacancy sharing ratio given by Meyerhof<sup>1</sup> fits the data well whereas the simple ratio of cross sections calculated by the binary encounter approximation does not. Thus the assertion that molecular processes are important is affirmed.

<sup>1</sup>W. E. Meyerhof, Phys. Rev. Lett. 31, 1341 (1975).

(C. W. Woods, R. L. Kauffman, K. A. Jamison, and P. Richard)

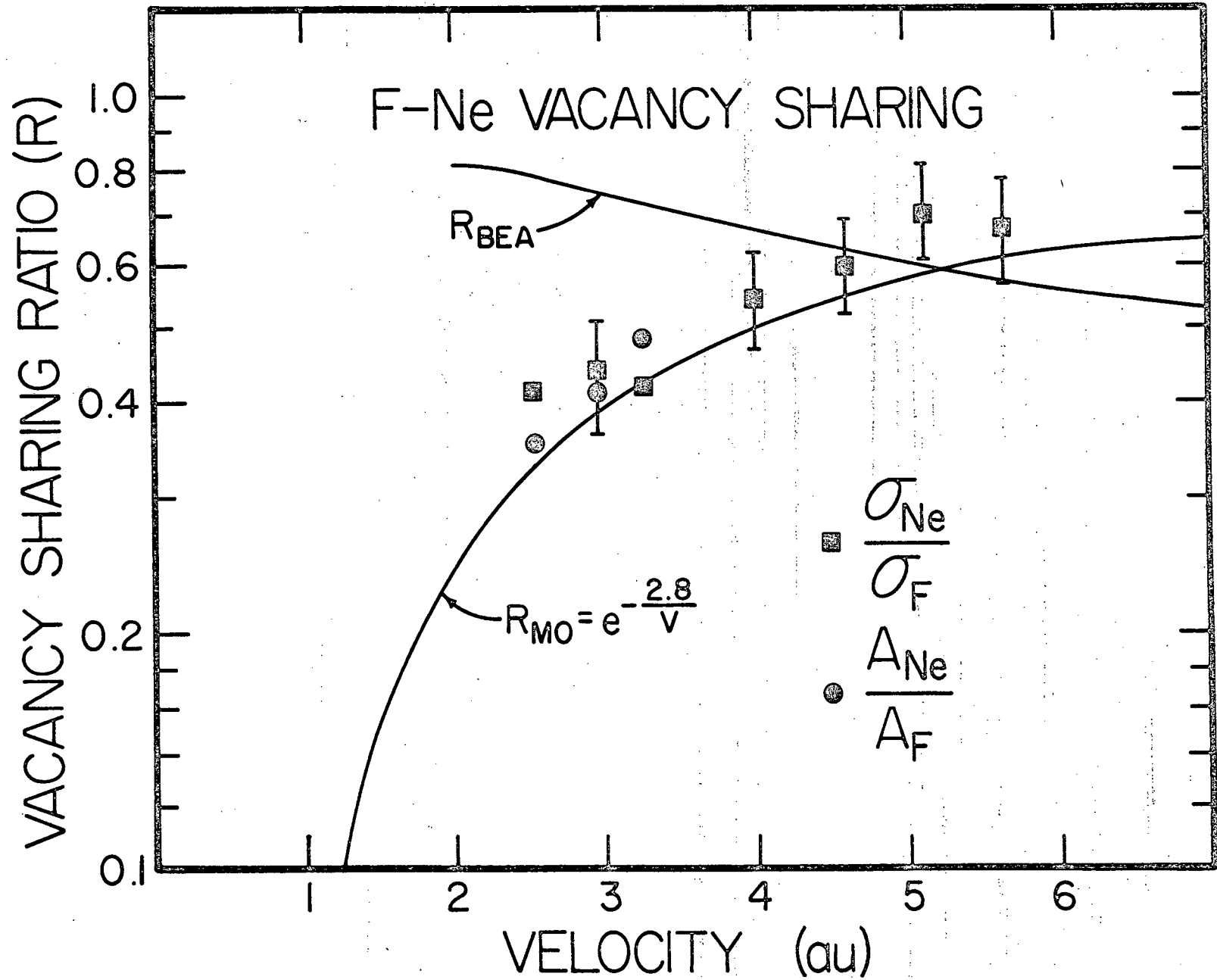


Fig. 1  
Sec. 3.6

### 3.7 K-Shell Auger Electron Hypersatellites of Ne

The cross section for production of excited Ne ions with double K-shell vacancies has been measured by observing the Auger electrons from the decay of these states. The K-shell Auger hypersatellites are observed only for bare nuclear projectiles of 1-2 MeV/amu N, O, and F. The energy dependence of the  $F^{9+}$  induced hypersatellite cross sections suggests a K-shell electron exchange mechanism, since the observed cross section is decreasing with increasing projectile energy in the region studied. The charge state dependence indicates that it is necessary to have two K-shell vacancies present in the projectile to produce an appreciable amount of hypersatellite intensity. Resolution was not sufficient to resolve the estimated 130 allowed KLM and KLL Auger hypersatellite transitions but total intensities could be extracted. The KLL hypersatellites result in 15% of the Auger spectrum and the KLM excitation hypersatellites account for 5% of the total spectrum for 30 MeV  $F^{9+}$ . The enhancement of a Li-like single K-shell vacancy Auger transition coinciding with the hypersatellite enhancement is reported. This is significant in that a configuration with four L-shell electrons or three L-shell electrons and one M-shell electron would feed the initial state of the Li-like transitions by KLL and KLM hypersatellite Auger decay. The importance of Auger-electron hypersatellites is pointed out as a necessary consideration in determining experimental fluorescence yield for ion-atom collisions involving bare nuclear projectiles.

(C. W. Woods, R. L. Kauffman, K. A. Jamison, N. Stolterfoht, and P. Richard)

### 3.8 Argon K-Auger Cross Sections in Collisions with 30 MeV F Ions

The cross sections for the production of argon K-Auger electrons by 30 MeV fluorine projectiles in charge states  $+5$  through  $+9$  are measured. By comparing these cross sections with previously measured x-ray production cross sections ( $\sigma_x$ ), K-shell fluorescence yields ( $\omega_K$ ) characterizing these collisions are deduced. Observed values of  $\omega_K$  average 11% above the neutral argon atom fluorescence yield and show no systematic dependence on projectile charge state. The results are summarized in the table below.

Projectile	E (MeV)	$(10^{-20} \text{ cm}^2)$		
		$\sigma_a^a$	$\sigma_x$	$\omega_K^a$
H <sup>+</sup>	4	0.604 <sup>b</sup>	0.0839 <sup>c</sup>	( $\equiv$ .122 <sup>d</sup> )
F <sup>+5</sup>	30	10.7	(1.59) <sup>e</sup>	.129
F <sup>+6</sup>	30	9.5	1.59 <sup>e</sup>	.143
F <sup>+7</sup>	30	14.9	2.49 <sup>e</sup>	.143
F <sup>+8</sup>	30	34.8	5.16 <sup>e</sup>	.129
F <sup>+9</sup>	30	64.1	10.2 <sup>e</sup>	.137
				$\bar{\omega}_K(\text{F}) = .136$

a) Estimated uncertainty 10% in  $\sigma_a$ ; 15% in  $\omega_K$

b) From  $\sigma_x = 0.0839$  and  $\omega_K = .122$ .

L. W. Winters, J. R. Macdonald, M. D. Brown, L. D. Ellsworth, and T. Chiao, Phys. Rev. A7, 1276 (1973).

c) Values from above reference multiplied by 1.10.

d) W. Bambynek, B. Crasemann, R. W. Fink, H. U. Freund, H. Mark, C. D. Swift, R. E. Price and P. Venugopala Rao, Rev. Mod. Phys. 44, 716 (1972).

L. M. Winters, J. R. Macdonald, M. D. Brown, T. Chiao, L. D. Ellsworth and E. W. Pettus, Phys. Rev. A8, 1835 (1973).

e) Values from above reference multiplied by 1.34;  $\sigma_x(^{+5})$  taken =  $\sigma_x(^{+6})$ .

(C. L. Cocke, R. R. Randall, and B. Curnutte)

### 3.9 Neon K Fluorescence Yields for $N^{Q+}$ -Induced Collisions

The Ne K Auger electron cross section for  $N^{4+,5+,6+,7+}$  bombardment at 14 and 19 MeV energy are measured. Ne K fluorescence yields are derived using the reported Auger electron cross sections combined with previous x-ray cross section measurements. These fluorescence yields are compared to semi-empirical yields derived from high resolution x-ray spectra. A summary of the results is given in the following table.

Ne K Cross Sections [ $10^{-19} \text{ cm}^2$ ] and Fluorescence Yields for  $N^{Q+}$  Impact.

Q+	14 MeV			19 MeV			21 MeV	
	$\sigma_x^a$	$\sigma_A$	$\omega_K$	$\sigma_x^a$	$\sigma_A$	$\omega_K$	$\omega_K$	$\omega_K^b$
4	0.94	11.5	0.076	1.02	14.5	0.066	0.060	0.034
5	1.35	22.2	0.057	1.49	28.4	0.050	0.046	...
6	3.67	50.4	0.068	3.10	50.3	0.058	0.055	0.046
7	12.53	83.2	0.131	8.11	84.3	0.088	0.079	9.078

a) F. Hopkins, R. Brenn, A. R. Whittemore, N. Cue, V. Dutkiewicz, and R. P. Chaturvedi, to be published in Phys. Letters A.

b) R. L. Kauffman, C. W. Woods, K. A. Jamison, and P. Richard, Phys. Rev. A 11, 872 (1975a).

(Forrest Hopkins, C. W. Woods, R. L. Kauffman, K. A. Jamison, and Patrick Richard)

#### 4. IONIZATION CROSS SECTIONS IN THIN SOLID MATERIALS

##### 4.1 K-Shell X-Ray Production Cross Sections for $^{12}\text{C}$ , $^{14}\text{N}$ and $^{16}\text{O}$ on Thin Solid Targets.

K-shell x-ray production cross sections were measured for  $^{12}\text{C}$ ,  $^{14}\text{N}$  and  $^{16}\text{O}$  projectiles incident upon thin targets of Ni, Rb, Ag and Sb. The measurements were undertaken to provide tests of the extension of presently available theories for inner-shell ionization for light incident ions to heavy ions, where the ratio of the projectile ( $Z_1$ ) and target ( $Z_2$ ) atomic numbers obey the property of  $Z_1/Z_2 < 1$ . In this work  $Z_1/Z_2$  ranged from 0.12 to 0.29. The energy range of the experiment was chosen to give equal values of  $E_1/M_1$  for each projectile species from 0.4 to 2.4 MeV/amu in steps of 0.2 MeV/amu.

The results for the comparison of the theoretical calculations of the x-ray cross section to the data are shown in Fig. 1 for  $^{12}\text{C}$  on Ni. It is seen that the unperturbed calculations represented by the plane-wave Born approximation (PWBA), the binary-encounter approximation (BEA) and the semiclassical approximation (SCA) all overpredict the magnitude of the measured cross section for K-x rays in this case. This feature is typical of the elements studied in the present work. The inclusion of binding energy corrections and Coulomb deflection corrections in the PWBA (to give the PWBABC theory) yields an improvement in the agreement between the theory and data. Further improvement is obtained if, in addition, the high energy electron polarization perturbation is also considered as in the curve labeled PWBABCP.

$Ni + {}^{12}C$

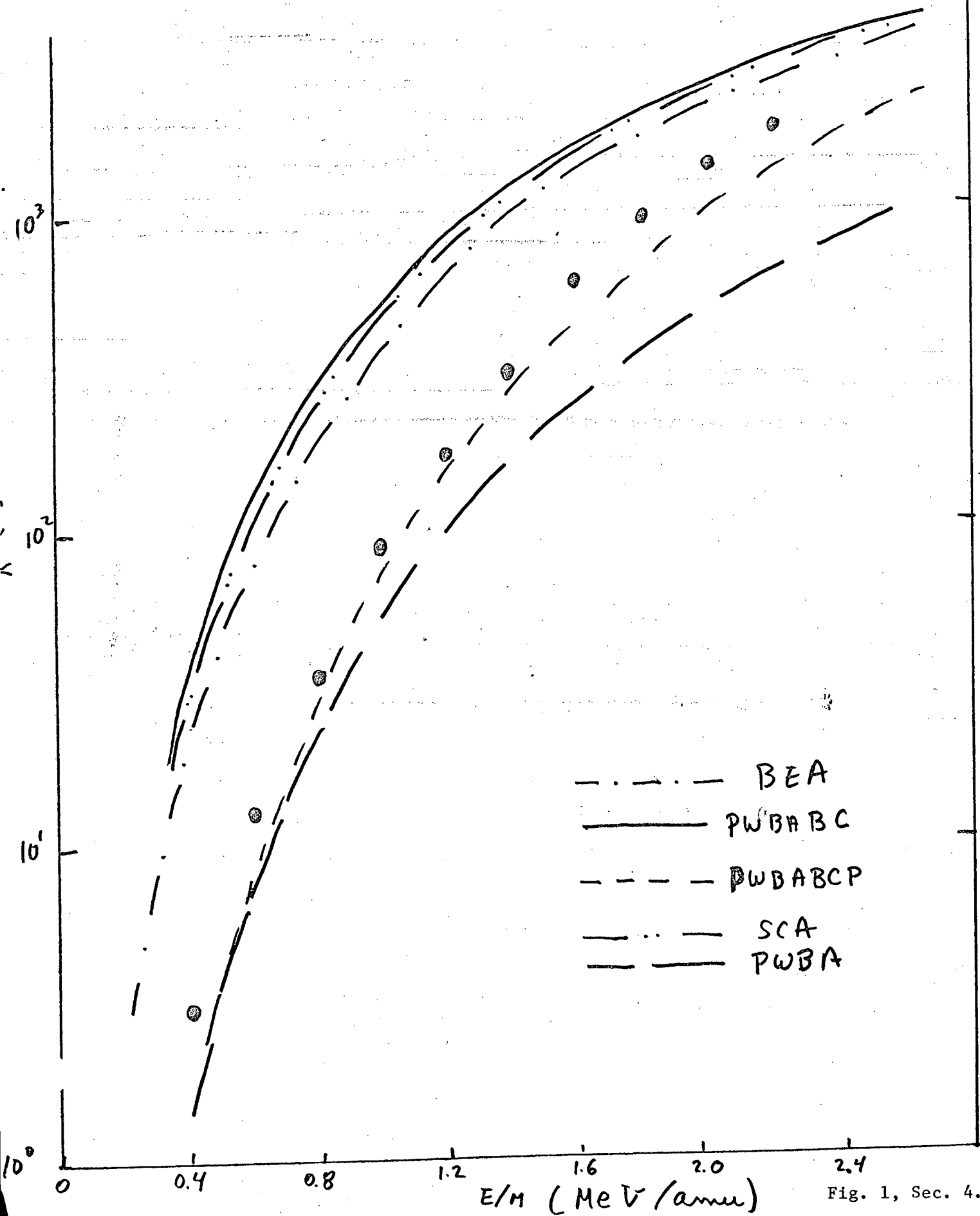


Fig. 1, Sec. 4.1

As the experiment was performed during one accelerator run, the relative cross sections for  $^{12}\text{C}$ ,  $^{14}\text{N}$  and  $^{16}\text{O}$  are independent of experimental normalizations for detector efficiencies and target configurations. A direct comparison of the x-ray production cross sections thus provides a critical test of the predicted  $Z_1^2$ -dependence of the unperturbed theories (PWBA, BEA and SCA). Shown in Fig. 2 is such a comparison for Ag bombarded by  $^{12}\text{C}$ ,  $^{14}\text{N}$  and  $^{16}\text{O}$ . The data are in excellent agreement with the predictions of the PWBABC theory in regards to the crossover in the cross section magnitudes, i.e., the  $^{16}\text{O}$ -induced cross section is lower than the  $^{12}\text{C}$ -induced cross section at the lower energies and the reverse is observed at the higher energies. Inspection of the causative factors for this behavior theoretically shows that the binding energy effect is solely responsible for such behavior with > 90% of the reduction in calculated cross section (compared to the PWBA) being directly associated with the binding energy perturbation.

Larkins' estimates<sup>1</sup> of the changes in the fluorescence yield,  $\omega_K$ , arising from multiple ionization show that  $\omega_K$  should not increase by more than 16% for the worse case (Ni). Such changes in  $\omega_K$  tend to raise the calculated cross sections and hence further and to the magnitude discrepancy for the unperturbed calculations. As the PWBABC calculations are  $\sim 50\%$  below the data @  $E_1/M_1 = 1.4 \text{ MeV/amu}$ , such changes in  $\omega_K$  will not account for the observed differences between the data and this theory.

Inclusion of the polarization effects does not lead to a resolution of the magnitude discrepancy for the PWBABC. Consideration of other mechanisms such as K-shell charge transfer may be appropriate. However,

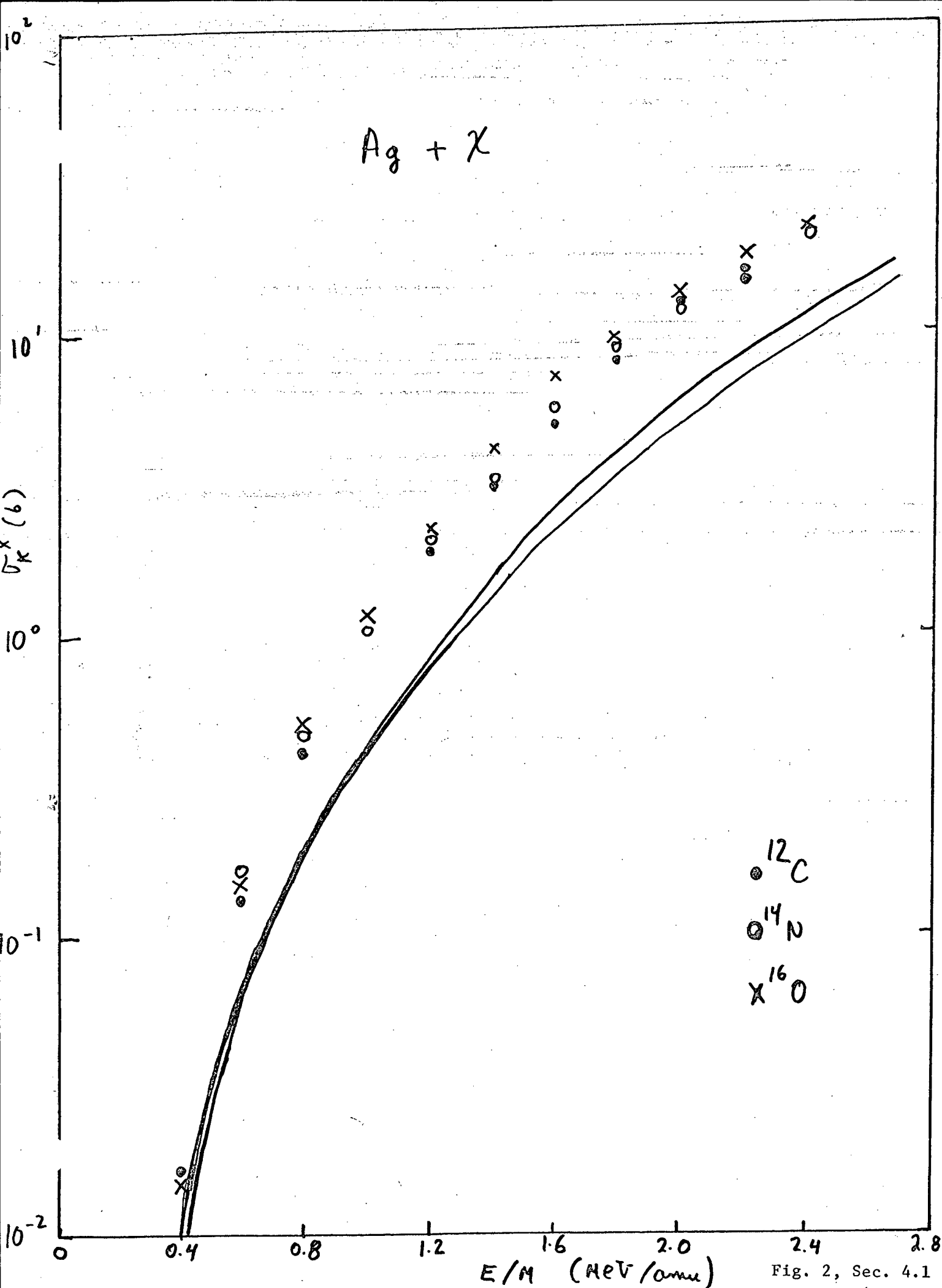


Fig. 2, Sec. 4.1

such comparisons are yet to be made and await an adequate theory for the purpose of comparison to the results such as are in the present work.

1) F. P. Larkins, J. Phys. B 4, L29 (1971).

(Tom J. Gray, Patrick Richard, Robert L. Kauffman, R. K. Gardner, G. M. Light, T. C. Holloway and J. Guertin)

#### 4.2<sup>2</sup> High Resolution Studies of L-Shell Ionization by Light Ions.

Work is in progress on the measurement of transition strengths for the L-x-rays arising from light ion bombardment. The work is planned for the incident ion species  $^1\text{H}$ ,  $^4\text{He}$  and  $^9\text{Be}$ . This work may allow the observation of entrance channel effects on the relative radiative widths of transitions involving equivalent final states. As the observed radiative strengths for transitions such as  $L_n$  and  $L_{\gamma_1}$  which are  $L_{II}$ -transitions depend upon the  $M_I$  and  $N_{IV}$  electron population, respectively, measurements of their relative radiative widths is proportional to the integration of the projectile with the outer shell electrons independent of the  $L_{II}$ -hole formation.

Preliminary work has been completed to optimize the experimental parameters associated with instrumental resolution, target configuration, and count rate. Modifications to existing target facilities now allow absolute normalization to the scattered projectile yield arising from nuclear elastic scattering. Work is presently in progress to allow absolute

efficiency calibration of the crystal spectrometer by use of a calibrated Si(Li) detector.

(Tom J. Gray, Patrick Richard, Keith Jamison and Jim Hall)

#### 4.3 M-Subshell X-Ray Cross Section Measurements.

Work is in progress on the measurements of M-shell x-ray cross sections for protons on Au. Thin self-supporting targets of Au have been bombarded with protons over an energy range of 2.6 to 5.0 MeV. The  $M_{3-N_1}$ ,  $M_\alpha$ ,  $M_\beta$  and  $M_\gamma$  relative x-ray cross sections have been measured and work is in progress to determine the absolute efficiency of the ARL 25600 spectrometer in order to obtain absolute x-ray cross section values. The measured transitions allow the study of the  $M_{III^-}$ ,  $M_{IV^-}$  and  $M_V^-$  ionization cross sections through the x-ray channel, thereby providing a basis for tests of the PWBA theory for M-shell ionization. It is planned to extend the bombarding energy range down to  $\sim 0.4$  MeV, in order to examine the predicted structure in the  $M_{III^-}$ -related x-ray transitions as a function of incident projectile energy. Further work with  $^4\text{He}$  and  $^9\text{Be}$  is planned to examine the need for perturbation corrections to the PWBA theory and the systematic properties of M-shell ionization for ions other than  $^1\text{H}$ .

(Tom J. Gray, Patrick Richard, Keith Jamison, and Jim Hall)

## 5. EXPERIMENTAL IMPACT-PARAMETER DEPENDENT PROBABILITIES FOR K-SHELL VACANCY PRODUCTION BY FAST HEAVY-ION PROJECTILES

The impact parameter dependence of the probability for production of target K x rays has been measured for oxygen projectiles on copper and for carbon and fluorine projectiles on argon at scaled velocities near 0.5. The O-on-Cu data was taken for 1.56, 1.88 and 2.69 MeV/amu O beams incident upon thin Cu foils. A thin Ar gas target was used for 1.56 MeV/amu C and F beams, permitting measurements to be made for charge-pure  $C^{+4}$ ,  $C^{+6}$ ,  $F^{+9}$ , and  $F^{+5}$  projectiles. Ar and Cu K x rays were observed in a Si(Li) detector and scattered projectiles in a collimated surface-barrier detector. Comparison of the shapes of the measured probability curves with predictions of the semi-classical Coulomb approximation (SCA) shows adequate agreement for the O-on-Cu system. For the higher ratio of projectile to target nuclear charge ( $Z_1/Z_2$ ) characterizing the C-on-Ar and F-on-Ar systems, the SCA predictions are entirely inadequate in describing the observed impact parameter dependence. In particular they cannot account for large probabilities found at large impact parameters. Further, the dependence of the shapes on the projectile charge state is found to become pronounced at the larger  $Z_1/Z_2$ . Fig. 1 depicts this trend for five measurements.

An attempt to account for this behavior in terms of a molecular-orbital vacancy-production process has been made. The approach used follows closely that discussed by Briggs and Taulbjerg (to be published). The time-dependent Schrödinger equation was integrated numerically for a system constrained to evolve within a basis of the  $1s\sigma$ ,  $2p\sigma$  and  $2p\pi$

orbitals. The rotational matrix element coupling the  $2p\sigma$  and  $2p\pi$  orbitals was approximated by  $\frac{bv}{R^2} e^{-Z_1 Z_2 (R/8)^2}$ . The radial matrix element coupling the  $1s\sigma$  and  $2p\pi$  orbitals was generated by extrapolating, from more nearly charge symmetric cases, the matrix elements calculated by Briggs and Taulbjerg. Initially the  $2p\sigma$  orbital (K-shell fluorine) was assumed vacant, the equations of motion were integrated with the projectile following a Coulomb trajectory, and the probability that the vacancy emerges from the encounter in the  $1s\sigma$  (K-shell argon) was evaluated.

The results are shown in Fig. 2. Since, for  $F^{+5}$  on Ar the  $2p\sigma$  is presumably initially filled, we take the difference between the  $P(b)$  curves for  $F^{+5}$  and  $F^{+9}$  to represent the experimental measure of  $1s\sigma - 2p\sigma$  vacancy transfer. There is no agreement between experimental and calculated curves. However, there are features of the calculation which deserve attention. The model produces an oscillatory behavior of  $P(b)$  not observed experimentally. This oscillation, in both  $b$  and  $v$ , results from the coherence between the  $1s\sigma - 2p\sigma$  transfer on incoming and outgoing paths. That is, the vacancy transfers from  $2p\sigma$  to  $1s\sigma$  going in but partially transfers back going out. The probability for finding the vacancy in the  $1s\sigma$  orbital is much larger halfway through the collision than it is after the entire encounter is completed. In fact, if one artificially suppresses the re-transfer by evaluating  $P(b)$  at the distance of closest approach, one obtains a  $P(b)$  which closely resembles the experimental one, as shown in Fig. 2.

(R. R. Randall, J. A. Bednar, B. Curnutte and C. L. Cocke)

VACANCY PRODUCTION PROBABILITY per COLLISION

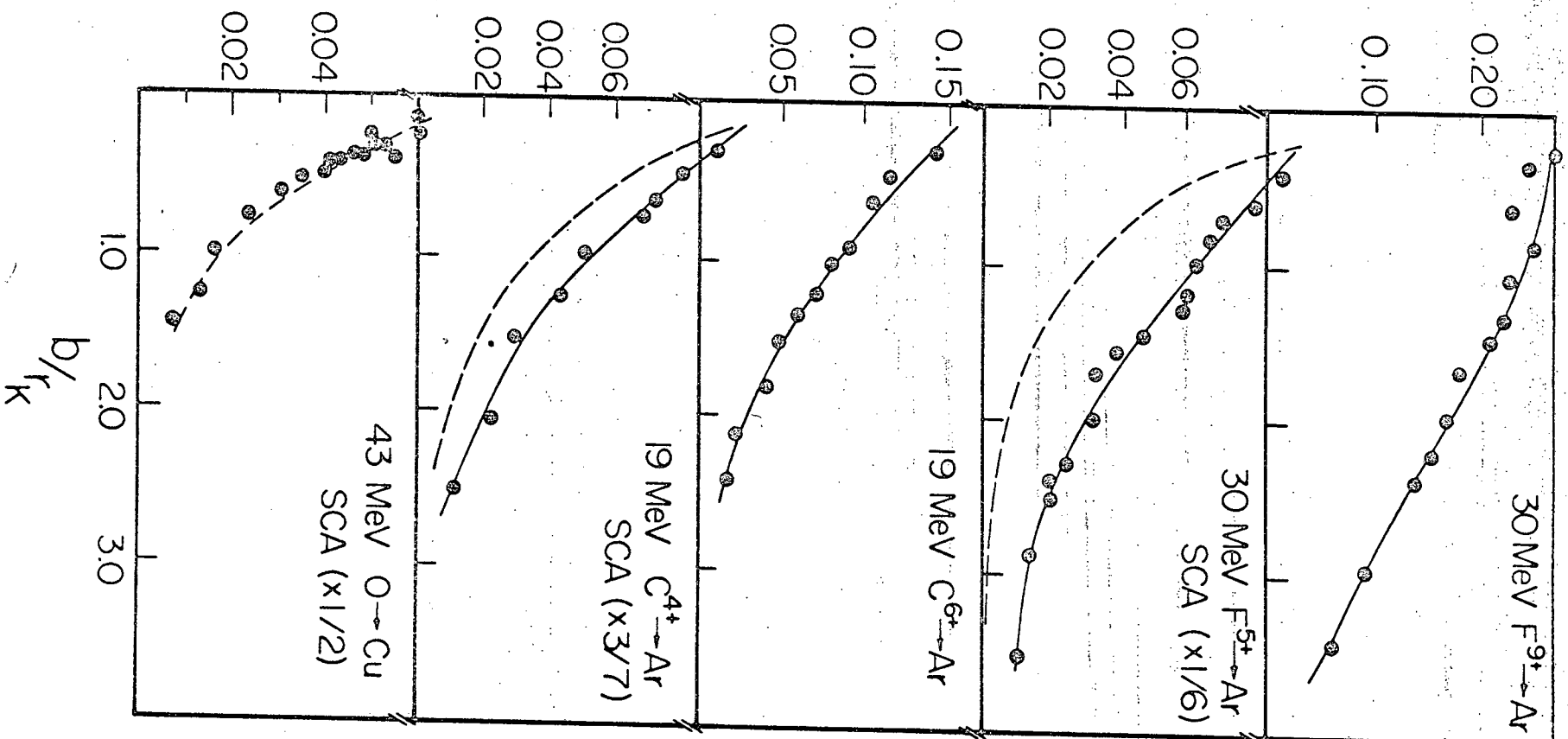


Fig. 1  
Sec. 5

VACANCY PRODUCTION PROBABILITY per COLLISION

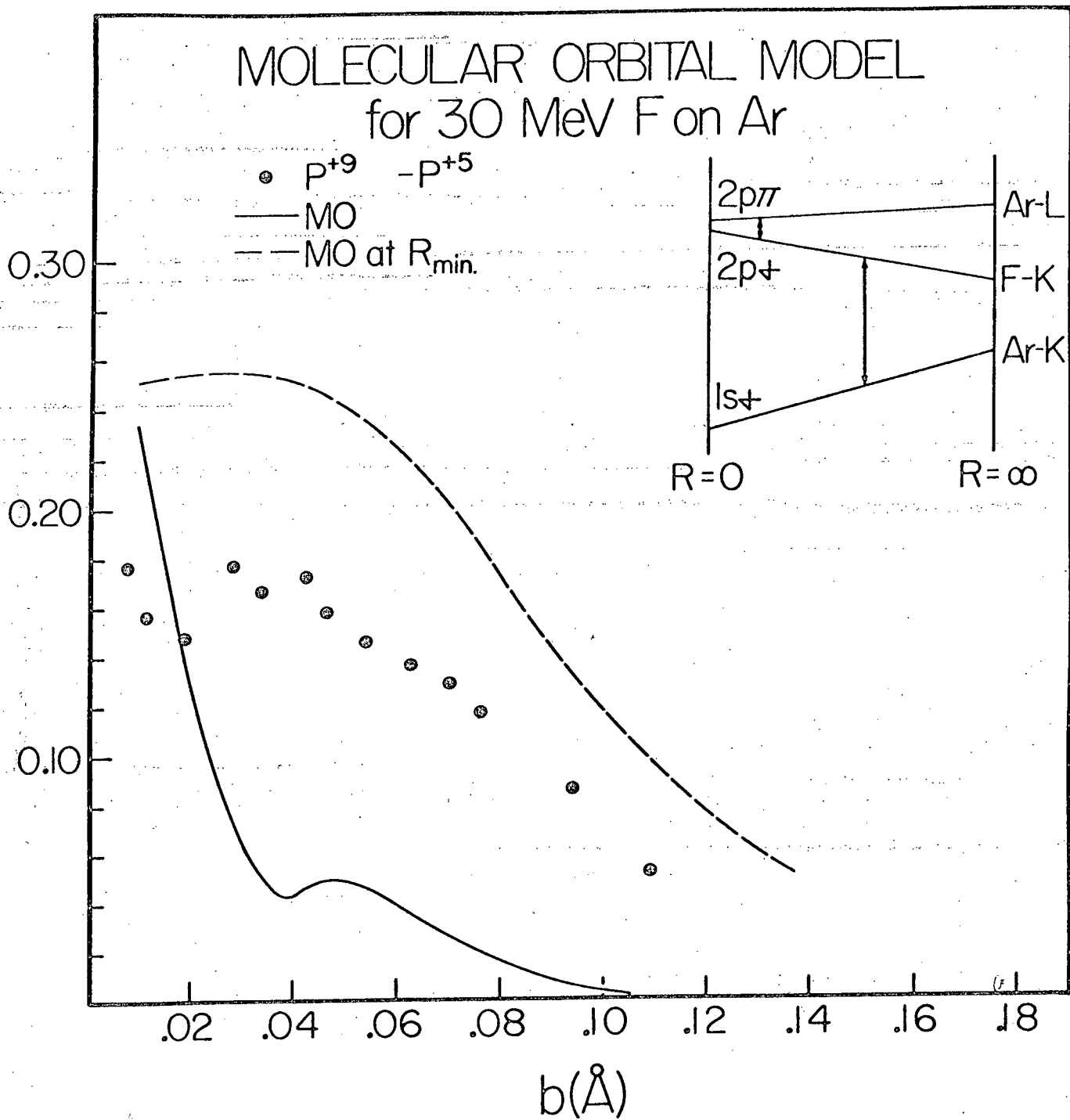


Fig. 2.  
Sec. 5

## 6. X-RAY SPECTROSCOPY WITH HIGH ENERGY IONS

### 6.1 Radiative Auger Effect in Ion-Atom Collisions

The radiative Auger effect, RAE, has been observed for Al and Si bombarded by 1-2 MeV  $H^+$ . This is the first observation of the RAE x-ray edge using ion excitation. Since the RAE is a fundamental mode of decay it should be independent of the method of excitation. The RAE has been observed previously in high resolution x-ray spectra of primary and secondary excitation.<sup>1</sup> The observance of the RAE in  $H^+$  induced spectra adds support to the hypothesis that the RAE is a fundamental mode of decay.

The RAE x-ray structure which falls 91 and 124 eV below the energy of the  $K\alpha_{1,2}$  line in Al and Si respectively is approximately 0.15% of the normal  $K\alpha$  x-ray intensity. These structures occur at the same energy and with the same relative intensity for  $H^+$  induced spectra as for electron and photon excitation. The most prominent of these structures is an edge corresponding to the  $K-L_{23}L_{23}$  Auger energy which is consistent with the RAE theory.

<sup>1</sup>J. Siivola, J. Ultriainen, M. Linkoaho, G. Graeffe, and T. Aberg, Phys. Lett. 32A, 458 (1970).

(P. Richard, J. Oltjen, K. A. Jamison, R. L. Kauffman, C. W. Woods, and J. M. Hall)

## 6.2 Radiative Electron Rearrangement: A Proposed Description for Low Energy Satellites Observed in Ion-Atom Collisions

We propose a satellite sequence as an explanation for the low intensity peaks observed just below the energy of the  $K\alpha_{1,2}$  normal x-ray line. The sequence arises from the radiative decay of the  $(1s)^{-1}(2p)^{-n}$  initial configuration to the  $(2s)^{-2}(2p)^{-n+1}$  final configuration. In this rearrangement process the 1s and one of the 2p vacancies are simultaneously filled by the 2s electrons, and a single photon is emitted. Since this model requires at least one L-shell vacancy in addition to the K-shell vacancy, the yield for  $H^+$  and  $e^-$  induced spectra should be small however a much larger yield is expected for heavy-ion collisions were single K-multiple L-shell vacancy populations are more probable. Hartree-Fock energies for this rearrangement decay agree well with the observed radiative electron rearrangement peaks ( $n = 1-4$ ) for target  $Z$  from Na to Ti.

(Keith A. Jamison, Jim Hall, and Patrick Richard)

### 6.3 Enhancement of Radiative Electron Rearrangement in Si by He<sup>+</sup> Bombardment

It has been shown that the energies of the peaks observed below the  $K\alpha_{1,2}$  line can be predicted by radiative electron rearrangement (RER) in the K and L shells (see previous section). In this model two sequences of lines based on the  $(1s)^{-1}(2p)^{-n}$  initial configuration are predicted. One sequence is the normal  $K\alpha L^n$  satellite decay to the  $(2p)^{-(n+1)}$  final configuration. The other sequence is the competing RER decay branch to the  $(2s)^{-2}(2p)^{-(n-1)}$  final configuration. Spectra induced by  $e^-$  and  $H^+$  show the radiative Auger effect (RAE) edge as well as the first ( $n = 1$ ) RER satellite ( $RER_1$ ). We have observed in He induced x-ray spectra of Si an order of magnitude increase in the intensity of  $RER_1$  as well as  $K\alpha L^1$  relative to  $K\alpha_{1,2}$ . This simultaneous enhancement of  $RER_1$  and  $K\alpha L^1$  gives support for the proposed RER model since the two transitions are decay branches of the same initial configuration. Si x-ray spectra obtained with  $H^+$  and  $He^+$  bombardment are shown in Fig. 1. The  $K\alpha L^n$  and  $RER_n$  x-ray branches are easily observed and identified. The measured branching ratios are  $RER_1/K\alpha L^1 = 0.14$  and  $0.18$  for  $H^+$  and  $He^+$  respectively and  $RER_2/K\alpha L^2 = 0.33$  for both  $H^+$  and  $He^+$  bombardment.

(J. Oltjen, R. L. Kauffman, C. W. Woods, J. M. Hall, K. A. Jamison, and Patrick Richard)

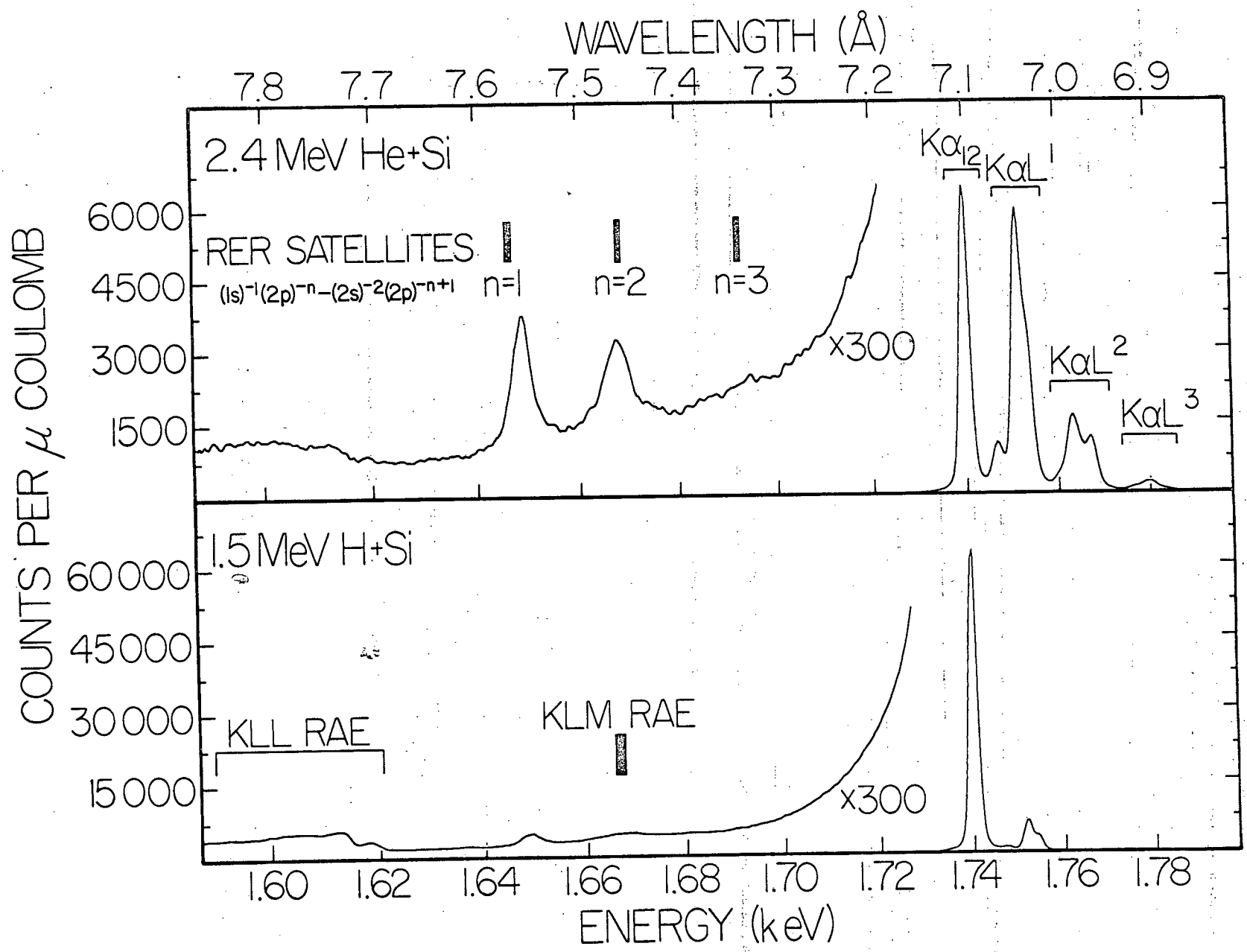


Fig. 1  
Sec. 6.3

#### 6.4 Multiplet Effects in High Resolution Ne K $\alpha$ Structure.

The effects of multiplet splitting upon high resolution Ne K x-ray spectra from ion-atom collisions are considered. The calculated splittings of the multiplets are as large as the splitting due to different charge states. The several multiplets, though, are grouped about a central value which is approximately the centroid of the observed peak. Special considerations must be given to the two- and three-electron systems due to (1) the small number of transitions with large multiplet splittings and (2) the population of the  $1s2s^2$  and  $1s2s$  configurations which have no K x-ray branches. The decay rates for the different decay channels for all of the different decays, especially the three-electron system, need to be calculated to interpret the K x-ray spectra. Bhalla recently has performed calculations for two multiplet levels for the doubly ionized case.<sup>1</sup> Despite the splitting effects and the effects of unobserved states, useful information concerning multiple ionization should be able to be obtained from the high resolution data.

<sup>1</sup>C. P. Bhalla, Phys. Lett. 46A, 185 (1973).

(R. L. Kauffman, C. W. Woods, K. A. Jamison, and P. Richard)

## 6.5 Charge-State Dependence of the Ne K Fluorescence Yield Deduced from High-Resolution Emission Spectra.

In this paper a method is described to determine semiempirical K fluorescence yields of Ne in ionization states  $KL^i$  for  $i = 1$  to 7. The method requires high-resolution K x-ray intensity ratios,<sup>1,2</sup> the K Auger-electron intensity ratio for the  $KL^0$  configuration,<sup>3,4</sup> and the average fluorescence yield<sup>5</sup> determined from x-ray and Auger-electron production cross sections. The analysis assumes that the ionization probability is described by a binomial distribution in the probabilities for single K-shell and single L-shell ionization.<sup>6,7</sup> Theoretical K fluorescence yields of Ne have been given by Bhalla and co-workers<sup>8</sup> and are found to increase with increasing L-shell ionization. In addition, Matthews *et al.*<sup>3</sup> have calculated semi-empirical fluorescence yields of Ne which differ from the values of Bhalla and co-workers and which are not independent of the projectile producing the ionization. In the present work we analyze the cases of 30-MeV  $O^{5+} + Ne$  and 35-MeV  $O^{8+} + Ne$  and obtain a set of fluorescence yields for ionization states  $KL^i$  which are consistent within the experimental errors. These are the only two cases for which enough data are available to obtain fluorescence yields by the present technique.

<sup>1</sup>R. L. Kauffman, F. Hopkins, C. W. Woods, and P. Richard, Phys. Rev. Lett. 31, 621 (1973).

<sup>2</sup>D. L. Matthews, B. M. Johnson, and C. F. Moore, Phys. Rev. A 10, 451 (1974).

<sup>3</sup>D. L. Matthews, B. M. Johnson, L. E. Smith, J. J. Mackey, and C. F. Moore, Phys. Lett. 48A, 93 (1974).

- <sup>4</sup>D. Burch, N. Stolterfoht, D. Schneider, H. Wieman and J. S. Risley, to be published.
- <sup>5</sup>D. Burch, W. B. Ingalls, J. S. Risley, and R. Heffner, Phys. Rev. Lett. 29, 1719 (1972); D. Burch, N. Stolterfoht, D. Schneider, H. Wieman, and J. S. Risley, Phys. Rev. Lett. 32, 1151 (1974).
- <sup>6</sup>D. Burch and H. Swanson, in Proceedings of the International Conference on Inner-Shell Ionization Phenomena and Future Applications, Atlanta, Georgia, 1972, edited by R. W. Fink, S. T. Manson, I. M. Palms, and P. V. Rao, CONF 720404 (U. S. AEC, Oak Ridge, Tennessee, 1973) p. 1464; I. M. Hansteen and O. P. Mosebekk, Phys. Rev. Lett. 29, 1361 (1972).
- <sup>7</sup>F. F. Hopkins, D. O. Elliott, C. P. Bhalla, and P. Richard, Phys. Rev. A 8, 2952 (1973), and references included in this paper.
- <sup>8</sup>C. P. Bhalla and M. A. Hein, Phys. Rev. Lett. 30, 39 (1973); C. P. Bhalla, N. O. Folland, and M. A. Hein, Phys. Rev. A 8, 649 (1973).

(N. Stolterfoht, D. Schneider, P. Richard and R. L. Kauffman)

#### 6.6 Relative Multiple Ionization Cross Sections of Neon by Projectiles in the 1-2 MeV/amu Energy Range.

The change in the K $\alpha$  x-ray spectra of neon is studied as a function of projectiles of C<sup>+3,+4,+5,+6</sup>, N<sup>+4,+6,+7</sup>, O<sup>+4,+5,+6,+7,+8</sup>, and F<sup>+9</sup> having an energy between 1 and 2 MeV/amu. The spectra are observed using a curved crystal spectrometer with a resolution of  $\sim 4$  eV. Combined with previous

measurements data are obtained for projectiles from carbon to argon. X rays are observed from different ionization states of Ne designated by  $KL^n$  for  $n = 1-7$ . An 81% correction between the  $KL^5$  peak and  $KL^6$  peak is derived. Semiempirical fluorescence yields are applied to the relative x-ray intensities to obtain relative multiple ionization cross sections. These cross sections are fitted by a binomial distribution as predicted by Coulomb ionization. All cases give good fits except for the  $F^{+9}$  induced spectra. A possible explanation is that a different excitation mechanism may exist for this near-symmetric collision case.

(Robert L. Kauffman, C. W. Woods, K. A. Jamison, and Patrick Richard)

#### 6.7 $K\alpha$ Satellite X Rays in Al, Sc, and Ti Following Bromine-Ion Bombardment.

A 4" curved crystal spectrometer has been used to resolve structure in  $K\alpha$  x rays from thick targets of Al, Sc, and Ti following bromine-ion bombardment. We have found that Br-induced spectra show structure that can be resolved into  $K\alpha L^n$  peaks. The  $K\alpha L^n$  peaks of Al are clearly resolved for  $n = 0-5$ , however the  $K\alpha L^n$  peaks of Sc and Ti are resolved only for states with  $n \geq 4$ . All peaks are broadened and shifted to higher than normal energy due to the degree of M-shell ionization. We can conclude that the M-shell ionization increases with L-shell ionization for Ti and Sc which is due to a collisional process and that M-shell ionization is nearly the same for these two targets. Al shows nearly equal relative

intensities for 2, 3, and 4 L-shell vacancies and exhibits a slight decrease in M-shell vacancies with increasing L-shell ionization.

(K. A. Jamison, C. W. Woods, Robert L. Kauffman, and Patrick Richard)

#### 6.8 Neon $K\alpha$ , $K\beta$ Satellite Structure Induced by 80-MeV Argon-Ion Impact

High-resolution (full width obtained half-maximum  $\sim 3$  eV) neon  $K$  x-ray spectra obtained with 80-MeV argon-ion bombardment from the Oak Ridge Isochronous Cyclotron are for two narrow ranges of the projectile charge state ( $q = \sim 6, \sim 14$ ). Production of the various satellite lines is found to depend on the projectile charge state. When the projectile is  $\text{Ar}^{14+}$ , the target is at least 6 times ionized, and a significant fraction ( $> 20\%$ ) of the observed radiation comes from hydrogenlike and heliumlike ions.

(J. Richard Mowat, Roman Laubert, I. A. Sellin, Robert L. Kauffman, Matt D. Brown, James R. Macdonald, and Patrick Richard)

## 7. ATOMIC LIFETIME MEASUREMENTS

### 7.1 Lifetime Measurement of the $^3P_1$ State of Heliumlike Sulphur

An apparatus suitable for direct beam-foil measurement of mean lives of x-ray emitting states with lifetimes in the neighborhood of  $10^{-12}$  sec has been developed. The apparatus uses a uniformly linear track which moves the exciting foil in steps of  $1.3 \mu\text{m}$ . A Doppler tuned spectrometer is used to observe radiation from the foil and up to  $1000 \mu\text{m}$  downstream. A  $5590 \text{ \AA}$  thick nickel foil was used with sulphur beams at 50, 60 and 66 MeV to obtain x-ray spectra of heliumlike sulphur.<sup>1</sup> The measured spatial resolution was approximately  $20 \mu\text{m}$ . The downstream edge of the foil position was assessed using the prompt Ni x rays from the foil. Our preliminary result for the lifetime of the  $^3P_1$  state in heliumlike sulphur is  $(1.7 \pm 0.3)$  psec in agreement with the theoretical value extrapolated from ref. 2.

<sup>1</sup>C. L. Cocke et al., Phys. Rev. A 9, 1823 (1974).

<sup>2</sup>G. W. F. Drake and A. Dalgarno, Ap. J. 157, 459 (1969).

(S. L. Varghese, C. L. Cocke, B. Curnutte, and R. R. Randall)

### 7.2 X-Rays from Foil-Excited Iodine Beams

M-X-ray spectra from foil-excited iodine beams between 40 and 62 MeV have been studied using a bent-crystal spectrometer. The prompt

spectrum is so rich as to defy analysis, but the delayed spectrum exhibits a number of resolved lines. Electric quadrupole  $4s \rightarrow 3d$  transitions are observed from metastable systems in the NiI, CuI and ZnI isoelectronic sequences. Electric dipole  $4p \rightarrow 3d$  transitions from states in these isoelectronic sequences also appear downstream. Transition energies and quadrupole lifetimes have been measured and are compared with the results of both relativistic and non-relativistic calculations. The line identification scheme is depicted in Fig. 1 which displays I beam x-ray spectra at two bombarding energies with the exciter foil just upstream of the viewed region. Fig. 2 gives the lifetime measurement data for the peaks labeled 1a, 2 and 3 in Fig. 1.

(C. L. Cocke, S. L. Varghese, J. A. Bednar, C. P. Bhalla, B. Curnutte, R. Kauffman, R. Randall, P. Richard, and C. Woods)

### 7.3 Lifetime of the $2^3S_1$ State in Heliumlike Sulphur and Chlorine

Beam-foil measurement of the lifetimes of the  $(1s2s) 2^3S_1$  state in heliumlike sulphur and chlorine have been made. A Doppler-tuned x-ray spectrometer was used to detect the x rays emitted from the  $1^1S_0 \leftarrow 2^3S_1$  transition. Time-of-flight techniques were used to trace the decay profile of the emitted x rays for 38-55-MeV sulphur and chlorine beams over flight paths of 56-861 cm. For foil-to-detector flight times greater than one half the theoretical lifetimes of 698 nsec (sulphur) and 374 nsec (chlorine),



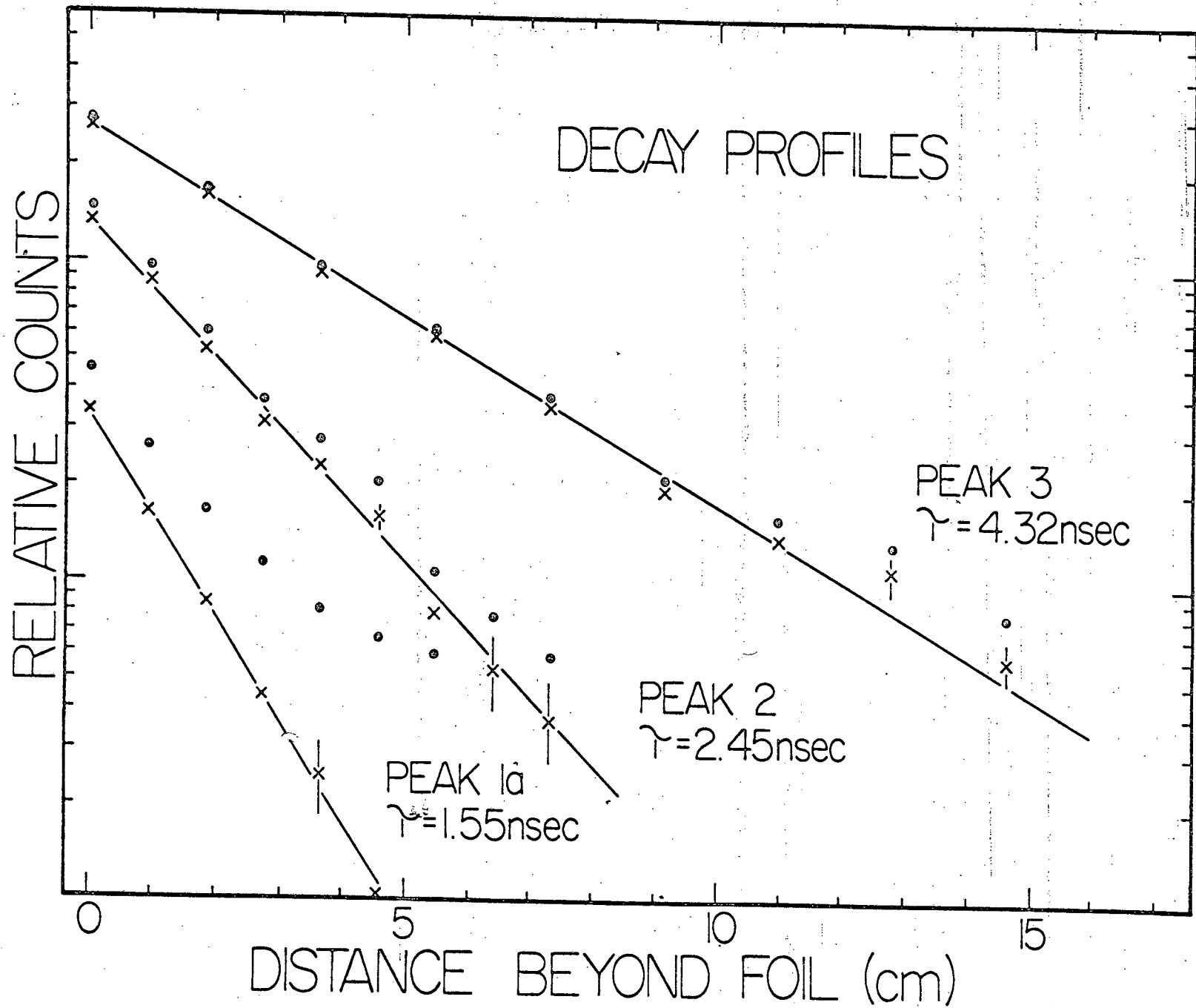


Fig. 2  
Sec. 7.2

the respective experimental lifetimes of  $706 \pm 86$  and  $354 \pm 24$  nsec are in agreement with theory. For shorter flight times, the experimental decay profiles are not single exponentials. This experimental effect is the source of the previously reported discrepancy between experimental and theoretical lifetimes of the  $2^3S_1$  state in heliumlike chlorine.

(J. A. Bednar, C. L. Cocke, B. Curnutte, and R. Randall)

## 8. POLARIZATION STUDIES OF ION-INDUCED X RAYS

### 8.1 Anisotropy of Characteristic K-Shell X Rays from Heavy-Ion-Atom Collisions.

Angular distributions of target and projectile K x rays have been measured for 3-MeV protons on Ar and 33-MeV  $F^{+6,+7,+9}$  on He and Ar. The Ar target K x-ray emission is nearly isotropic in all cases. The projectile K x-ray emission, however, is anisotropic in the moving frame of the projectile in all cases. A large polarization fraction,  $P$ , ( $\sim 23\%$ ) is deduced from the angular distribution formula for dipole radiation  $I(\theta) = I(90^\circ)(1 - P\cos^2\theta)$ , where  $\theta$  is the angle of emission in the emitting rest frame relative to the beam direction. The measured polarization fractions of the F projectile K x rays implies that the radiative P states are populated nonstatistically so as to favor  $m_l = 0$  over  $|m_l| = 1$  substate (defined by quantization along the beam direction). It is proposed that the polarization can be qualitatively understood as an alignment in excited states populated by electron capture in atomic collisions.

(E. H. Pedersen, S. J. Czuchlewski, M. D. Brown, L. D. Ellsworth, and J. R. Macdonald)

### 8.2 Polarization Fractions of K X Rays Emitted by Fast Fluorine Ions Incident in Different Charge States on He.

Polarization fractions as described in the previous section have

been measured for  $F^{n+}$  on He for the incident charge states  $n = 2-9$  at 10-MeV,  $n = 3-9$  at 19-MeV and  $n = 5-9$  at 30-MeV. The polarization fraction increases monotonically with  $n$  from a value of  $\sim 0.03$  to  $\sim 0.28$ . These results can be understood qualitatively if it is assumed that electron capture reactions produce alignment of excited states, while direct Coulomb ionization of a K electron leaves the rest of the ion in a state with no alignment. For low charge state ions, Coulomb ionization predominates and yields at most a small polarization fraction. With increasing charge state, contributions from electron exchange of K-shell ionization with simultaneous electron capture may explain increasing polarization fractions. For the bare nucleus case electron capture to excited states is the only excitation mechanism.

(S. J. Czuchlewski, L. D. Ellsworth, J. A. Guffey, E. H. Pedersen, E. Salzbom, and J. R. Macdonald)

### 8.3 Direct Measurement of the Linear Polarization of Lyman- $\alpha$ X Rays

The Bragg scattering from a convenient crystal can be used to investigate the polarization of x rays emitted following inner-shell ionization.<sup>1</sup> Such a polarimeter has been developed and used to measure directly the polarization of oxygen Lyman- $\alpha$  radiation emitted by energetic oxygen beams passing through a thin carbon foil. With no significant variation with beam energy from 8-32 MeV, a polarization fraction of  $(+14 \pm 2)\%$  was observed directly by comparing the radiation intensity in

the Bragg peak with the polarimeter oriented alternately parallel and perpendicular to the incident beam direction. The observed positive polarization that is attributed to electron capture processes is consistent with that deduced from anisotropic angular distributions of projectile x-radiation observed previously<sup>2</sup> in heavy-ion collisions.

<sup>1</sup>J. Hrdý, A. Henins, and J. A. Bearden, Phys. Rev. A 2, 1708 (1970).

<sup>2</sup>E. H. Pedersen et al., Phys. Rev. A 11, 1267 (1975);

S. J. Czuchlewski et al., Phys. Letters 51A, 309 (1975).

(L. D. Ellsworth, J. A. Guffey, J. R. Macdonald, and E. Salzbom)

## 9 THEORETICAL SPECTRA IN ION-INDUCED REACTIONS

### 9.1 Relative Multiple Ionization Cross Sections of Neon by Oxygen Ions

Several high-resolution studies of neon K x rays have been reported<sup>1-3</sup> for oxygen ions with bombarding energies  $\approx 1 - 2$  MeV/amu. The experimental peaks in the spectrum are usually labeled by the notation  $KL^n$ , implying a single K vacancy and  $n$  vacancies in the L-shell.

We made a reanalysis of x-ray data for 30 MeV  $O^{+5}$ -neon collisions. The theoretical fluorescence yields and transition energies<sup>4,5</sup> were used. We assume a statistical population of the spectroscopic terms and the binomial distribution for the relative population of the electronic configurations.<sup>3</sup> The theoretical x-ray relative intensities depend on the average probability of L-shell ionization at small impact parameters,  $P_L(0)$ . Figure 1 contains a theoretical x-ray spectrum for  $P_L(0)$  equal to 0.375. Each line was taken to be Gaussian<sup>†</sup> with a half-width,  $\Delta E$ , of 0.375 eV. It was found that the peaks labeled  $KL^6$ ,  $KL^5$ ,  $KL^4$ , and  $KL^3$  in the experimental studies<sup>1-3</sup> need corrections so that the relative x-ray intensities represent correctly the contributions of the various degrees of ionization, as indicated by the notation  $(KL^n)$ .

There are two high-resolution x-ray spectral measurements of neon for 30 MeV  $O^{+5}$  projectiles. The values of  $P_L(0)$  were obtained to be 0.375 and 0.345 respectively for the best fit to the experimental x-ray relative intensities as reported by Kauffman *et al.*<sup>3</sup> and by Matthews *et al.*<sup>2</sup> The theoretical x-ray spectrum for two values of  $P_L(0)$  are given in Fig. 2 by assigning a half width of 2 eV to each line. The

<sup>†</sup>  $I(E) = (\exp[-(E-E_0)/\Delta E]^2) / \Delta E \sqrt{\pi}$

X-RAY RELATIVE INTENSITY

5  
0  
5  
0

850

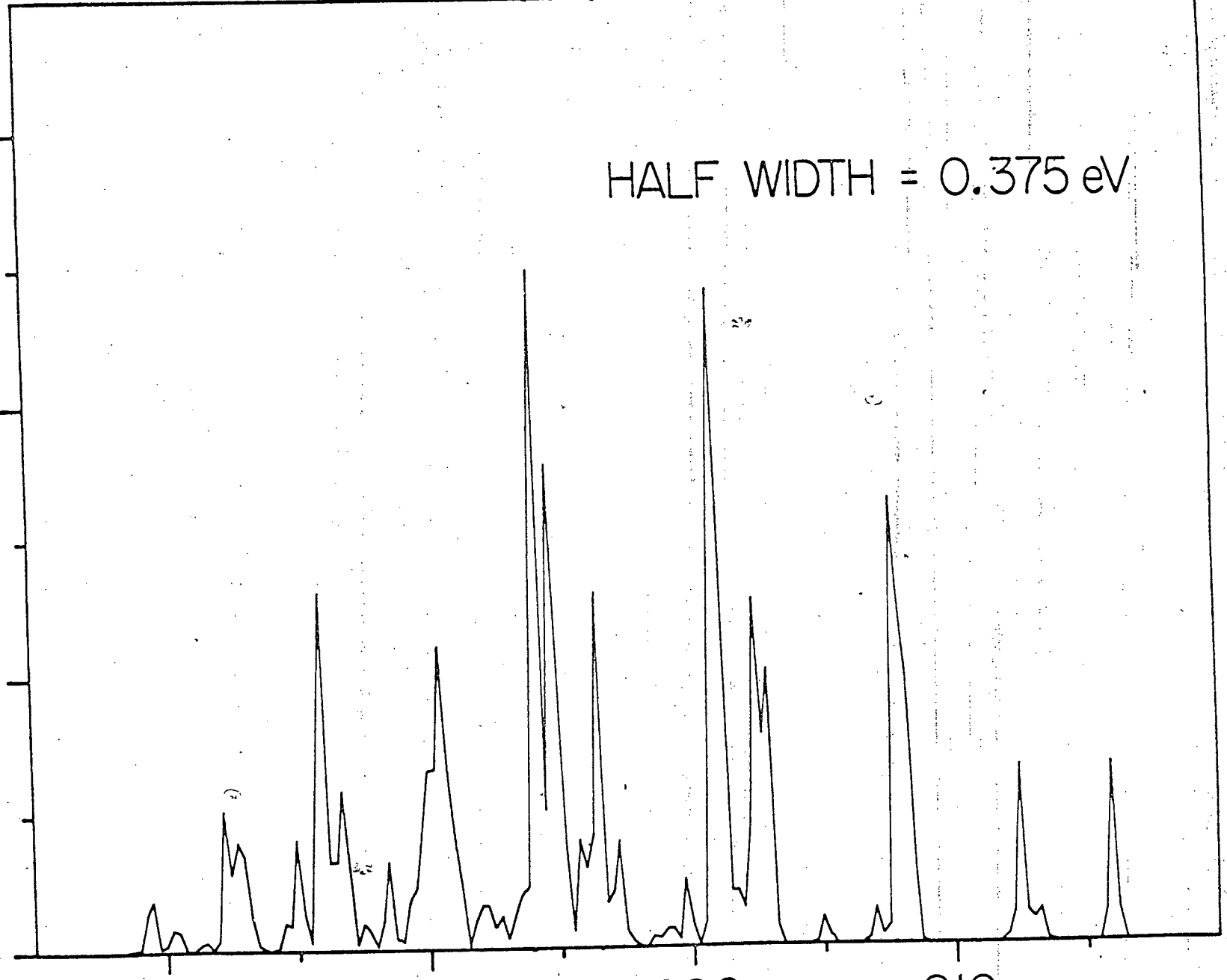
870

890

910

ENERGY (eV)

HALF WIDTH = 0.375 eV

Fig. 1  
Sec. 9.1

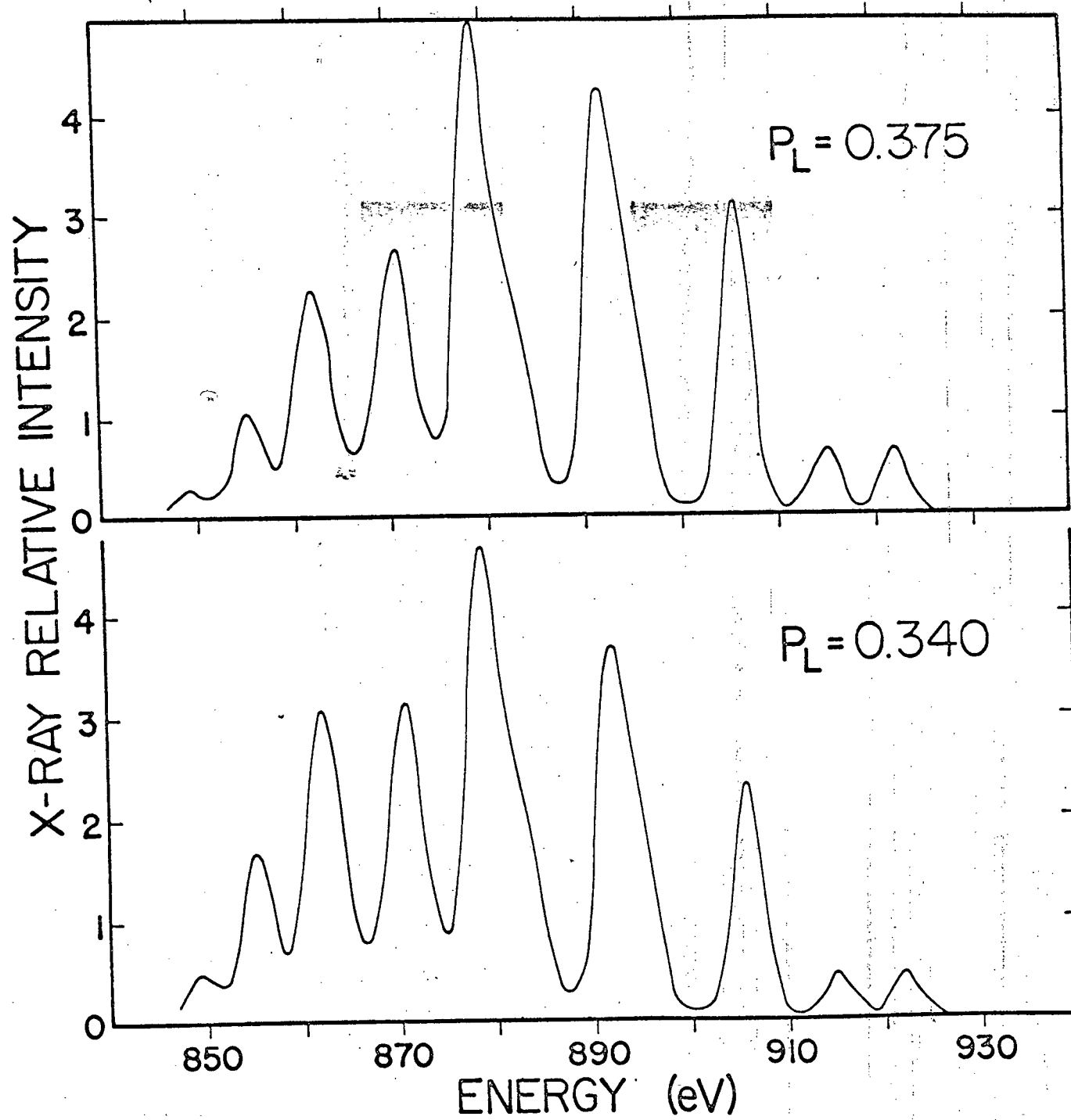


Fig. 2  
Sec. 9.1

relative ionization cross sections<sup>3,6</sup> are given by the following expression:

$$\sigma(KL^n)/\sigma(K) = \binom{8}{n} [P_L(0)]^n [1 - P_L(0)]^{8-n} ,$$

where  $\binom{8}{n}$  is the binomial coefficient. Using the theoretical fluorescence yields and values of  $P_L(0)$  as 0.375 and 0.340, we obtain the average fluorescence yields for 30 MeV  $O^{+5}$ -neon collisions respectively to be 0.045 and 0.038, which compare favorably with the experimental value<sup>7</sup> of  $0.04 \pm 0.008$ .

From our analysis it is clearly demonstrated that detailed calculations of the theoretical spectra averaged by a 2 eV Gaussian resolution reproduce the relatively simple experimental Ne spectra with 9 peaks. We conclude thus that the analyses of spectral measurements to obtain ionization cross sections should be performed by a direct comparison of the experimental and the theoretical relative intensities to avoid any errors and ambiguities arising from the overlap of multiplets belonging to different electronic configurations.

<sup>1</sup>R. L. Kauffman, F. F. Hopkins, C. W. Woods, and P. Richard, Phys. Rev. Letters 31, 621 (1973).

<sup>2</sup>D. L. Matthews, B. M. Johnson, C. F. Moore, Phys. Rev. A 10, 451 (1974).

<sup>3</sup>R. L. Kauffman, C. W. Woods, K. A. Jamison, and P. Richard, Phys. Rev. A 11, 872 (1975).

<sup>4</sup>C. P. Bhalla, Phys. Rev. A 12, 122 (1975).

<sup>5</sup>C. P. Bhalla, J. Phys. B 8 (1975).

<sup>6</sup>J. M. Hansteen and O. P. Mosebekk, Phys. Rev. Letters 29, 1361 (1972).

<sup>7</sup>D. Burch, W. B. Ingalls, J. S. Risley and R. Heffner, Phys. Rev. Letters 29, 1719 (1972).

(C. P. Bhalla)

## 9.2 Lifetimes and Fluorescence Yields of Three-Electron Ions

The theoretical investigations of few-electron ions are important for the diagnostic applications to plasmas and solar flares. Similarly such calculations are also relevant to the recent experimental spectral measurements in ion-atom collisions and the measurements of lifetimes.

Satellite lines situated on the long-wavelength side of helium-like resonance lines were first reported from laboratory spark sources by Edlén and Tyrén.<sup>1</sup> Walker and Rugg,<sup>2</sup> Parkinson,<sup>3</sup> Grineva et al.,<sup>4</sup> and Acton et al.,<sup>5</sup> published the experimental observations on the solar spectra. Grineva et al.<sup>6</sup> have now reported a new reduction of the iron XXV spectra and associated satellites, which are emitted during solar flares. Peacock et al.<sup>7</sup> and Feldman et al.<sup>8</sup> published the spectra from the laser-produced plasmas. Nagel<sup>9</sup> discussed x-ray diagnostics of laser-compressed plasmas. Golts et al.<sup>10</sup> have published a spectrum using a low inductance spark in iron.

The theory determining the wavelength and intensity of the lines for the heliumlike ions and ions with the  $1s\ 2p^2$ ,  $1s\ 2s^2$  and  $1s\ 2s\ 2p$

configurations is given by Gabriel and collaborators.<sup>11</sup> Recently Bhalla, Gabriel and Presnyakov<sup>12</sup> published the theoretical results on the dielectric satellite spectra for highly-charged helium-like ions. These calculations removed the most notable discrepancy reported previously for the satellite intensities.<sup>8</sup>

Sellin<sup>13</sup> has published an extensive review on the lifetimes of the  $4p^0_{5/2}$  autoionizing states of ions in the Li isoelectronic sequence. Calculations of Cheng et al.<sup>14</sup> are in reasonable agreement with the experimental data. More recently Betz et al.<sup>15</sup> have reported a new technique for measuring short lifetimes  $\approx 10^{-14}$  sec. Calculations of lifetimes for few-electron systems are, therefore, needed. Similarly, the line fluorescence yields,<sup>16</sup> defined as the ratio of the radiative rate for the line and the total rate for the level, are essential in the analysis of x-ray spectral measurements relevant to the heavy ion-atom collisions. Richard<sup>17</sup> and Macdonald<sup>18</sup> have recently reviewed this subject.

The calculations were performed in the intermediate coupling scheme and the configuration interaction between the  $1s 2s^2 2S$  and  $1s 2p^2 2S$  terms were included. The theoretical expressions for the autoionization rates in the L-S coupling are given below in atomic units ( $1 \text{ a.u.} = 2.419 \cdot 10^{-17} \text{ sec}$ ).

$$\begin{aligned}
 A_a(1s^2 \epsilon s \ 2S - 1s 2s^2 \ 2S) &= 2\pi[-R^0(1s, \epsilon s, 2s, 2s)]^2 \\
 A_a(1s^2 \epsilon s \ 2S - 1s 2p^2 \ 2S) &= \frac{2\pi}{3}[-R^1(1s, \epsilon s, 2p, 2p)]^2 \\
 A_a(1s^2 \epsilon d \ 2D - 1s 2p^2 \ 2D) &= \frac{2\pi}{15}[-R^1(1s, \epsilon d, 2p, 2p)]^2 \\
 A_a(1s^2 \epsilon p \ 2P - 1s 2p(3P) 2s^2 P) &= 3\pi[-R^0(1s, \epsilon p, 2s, 2p)]^2
 \end{aligned}$$

$$A_a(1s^2 \epsilon p^2 P - 1s2p(1P)2s^2 P) = 4\pi \left[ \frac{1}{3} R^1(1s, \epsilon p, 2p, 2s) - \frac{1}{2} R^0(1s, \epsilon p, 2s, 2p) \right]^2$$

The relative phases of the amplitudes are contained in the brackets.

The continuum electron of orbital angular momentum  $\ell$  is designated by  $\epsilon \ell$ .

The generalized Slater integrals involve three discrete states and one continuum state wavefunction. The detailed atomic model, Hartree-Fock-Slater with the HVDO exchange approximation, is described by Bhalla.<sup>16</sup>

The Hartree-Fock program of Froese-Fischer<sup>19</sup> was used to obtain the total energies of the various terms and the values of the spin-orbit parameters. The appropriate matrices for various values of the total angular momentum were diagonalized to obtain the eigenvectors and eigenvalues. The procedure of the adjustment of the calculated energies is discussed by Gabriel. All the appropriate radiative rates,  $A_r$ , and the autoionization rates were, then, calculated.

Table I contains the notation used for designating the individual lines. The wavelengths of the satellite lines are given by Gabriel, Vainstein and Safronova<sup>20</sup> and Goldsmith.<sup>21</sup>

The total rate,  $\Gamma_i$ , for a level ( $\alpha J_i$ ) is

$$\Gamma_i = \sum A_r + \sum A_a$$

where  $\sum$  denotes a sum over all transitions. The line fluorescence yield,  $\omega(\alpha J_i \rightarrow \alpha' J_f)$  is given by

$$\omega(\alpha J_i \rightarrow \alpha' J_f) = A_r(\alpha J_i \rightarrow \alpha' J_f) / \Gamma_i .$$

We have calculated the lifetimes of all the levels (a-v of Table I) of the  $1s\ 2p^2$ ,  $1s\ 2s^2$  and  $1s2s2p$  configurations and the line fluorescence yields for  $Z = 7, 8, 10, 16$  and  $26$ .

Table I: Key Letter System for Individual Lines

Array	Multiplet	Line	Key Letter
$1s^2 2p - 1s2p^2$	$2P^0 - 2P$	$1\frac{1}{2}-1\frac{1}{2}$	a
		$\frac{1}{2}-1\frac{1}{2}$	b
		$1\frac{1}{2}-\frac{1}{2}$	c
		$\frac{1}{2}-\frac{1}{2}$	d
	$2P^0 - 4P$	$1\frac{1}{2}-2\frac{1}{2}$	e
		$1\frac{1}{2}-1\frac{1}{2}$	f
		$\frac{1}{2}-1\frac{1}{2}$	g
		$1\frac{1}{2}-\frac{1}{2}$	h
	$2P^0 - 2D$	$\frac{1}{2}-\frac{1}{2}$	i
		$1\frac{1}{2}-2\frac{1}{2}$	j
	$2P^0 - 2S$	$1\frac{1}{2}-2\frac{1}{2}$	k
		$\frac{1}{2}-1\frac{1}{2}$	l
$1\frac{1}{2}-\frac{1}{2}$		m	
$\frac{1}{2}-\frac{1}{2}$		n	
$1s^2 2p - 1s2s^2$	$2P^0 - 2S$	$1\frac{1}{2}-\frac{1}{2}$	o
		$\frac{1}{2}-\frac{1}{2}$	p
$1s^2 2s - 1s2p2s$	$2S - (1P)2P^0$	$\frac{1}{2}-1\frac{1}{2}$	q
		$\frac{1}{2}-\frac{1}{2}$	r
	$2S - (3P)2P^0$	$\frac{1}{2}-1\frac{1}{2}$	s
		$\frac{1}{2}-\frac{1}{2}$	t
	$2S - 4P^0$	$\frac{1}{2}-1\frac{1}{2}$	u
		$\frac{1}{2}-\frac{1}{2}$	v
		$\frac{1}{2}-2\frac{1}{2}$	v'

<sup>1</sup>B. Edlén and F. Tyrén, Nature 143, 940-1 (1939).

<sup>2</sup>A. B. C. Walker and H. R. Rugg, Astrophys. J. 164, 181 (1971).

- <sup>3</sup>J. H. Parkinson, *Nature* 236, 68 (1972).
- <sup>4</sup>Yu Grineva, V. I. Darev, V. V. Korneyev, V. V. Krutov, S. L. Mandelstam, L. A. Vainstein, B. N. Vasilyev, and I. A. Zitnik, in Space Research XII (Akademie-Verlag, Berlin) 1972.
- <sup>5</sup>L. W. Acton, R. C. Catura, A. J. Meyerott, C. J. Wolfson, and J. L. Culhane, *Solar Physics* 26, 183 (1972).
- <sup>6</sup>Yu Grineva, V. I. Karev, V. V. Korneyev, V. V. Krutov, S. L. Mandelstam, L. A. Vainstein, B. N. Vasilyev, and I. A. Zitnik, *Solar Physics* 29, 441 (1973).
- <sup>7</sup>N. J. Peacock, M. G. Hobby, and M. Galanti, *J. Phys. B* 6, L298 (1973).
- <sup>8</sup>U. Feldman, G. A. Doscheck, D. J. Nagel, R. D. Cowan, and R. R. Whitlock, *Astroph. J.* 192, 213 (1974).
- <sup>9</sup>D. J. Nagel, *Physica Fennica* 9, Supplement S1, 403 (1974).
- <sup>10</sup>E. Ya Golts, I. A. Zhitnik, E. Ya Kononov, S. L. Mandelstam, and Yn. V. Sidelnikov, Report No. 4 of the Spectroscopy Institute, USA Academy of Sciences (to be published in *Soviet Physics, Doklady*) 1974.
- <sup>11</sup>A. H. Gabriel, *Mon. Not. R Astr. Soc.* 160, 99 (1972); A. H. Gabriel, and C. Jordan, in *Case Studies in Atomic Collision Physics - II*, eds, McDaniel and McDowell (North Holland); A. H. Gabriel, T. M. Paget, and H. J. Kunze, to be submitted to *J. Phys. B.*
- <sup>12</sup>C. P. Bhalla, A. H. Gabriel, and L. P. Presynakov, *Mon. Not. R. Astro. Soc.* 172, 359 (1975).
- <sup>13</sup>I. A. Sellin, *Nucl. Instr. & Methods* 110, 447 (1973).
- <sup>14</sup>K. Cheng, C. Lin, and W. R. Johnson, *Phys. Lett.* 48A, 437 (1974).

- <sup>15</sup>H. D. Betz, F. Bell, H. Panke, G. Kalkoffen, M. Welz, and D. Evers, Phys. Rev. Lett. 33, 807 (1974); H. D. Betz, H. Panke, and F. Bell, Intn'l Conf. on the Physics of Electronic and Atomic Collisions, Seattle, USA (1975).
- <sup>16</sup>C. P. Bhalla, Phys. Rev. A 12, 122 (1975).
- <sup>17</sup>P. Richard, in Atomic Inner-Shell Processes, ed. B. Crasemann (Academic Press), Vol. I.
- <sup>18</sup>J. R. Macdonald, Intn'l Conf. on the Physics of Electronic and Atomic Collisions, Seattle, USA (1975) (invited talk).
- <sup>19</sup>C. Froese-Fischer, Comp. Phys. Comm. 1, 15L (1960).
- <sup>20</sup>L. A. Vainstein and U. I. Safronova, Short Communications in Physics 3, 40 (1972) (Lebedev Institute, Moscow).
- <sup>21</sup>S. Goldsmith, J. Phys. B 7, 2315 (1974).

(C. P. Bhalla and A. H. Gabriel)

### 9.3 Relativistic Contributions to Transition Energies in NiI and CuI Isoelectronic Sequences.

Since the compilation of Moore,<sup>1</sup> the NiI isoelectronic sequence has been studied up to Z=42 by Alexander et al. and for Z=62, 64, and 66 by Burkhalter et al. Only electric dipole decays were observed. Measurement of transition energies for  $3d^9 4f \rightarrow 3d^{10}$  and  $3d^9 4p \rightarrow 3d^{10}$  lines as high as Z=66 allows one to construct formulae for interpolating with rather good confidence to energies in the NiI sequence for intermediate Z.

No detailed equivalent information appears to be available for the  $3d^9 4s \rightarrow 3d^{10}$  quadrupole decays for  $Z$  above 33. Cocke et al.<sup>2</sup> have reported recently the M-x-ray spectra from foil-excited iodine beams. The electric quadrupole  $4s \rightarrow 3d$  and the electric dipole  $4p \rightarrow 3d$  transitions of multiply-ionized iodine were studied in the NiI, CuI and ZnI isoelectronic sequences. The relativistic contributions to the transition energies were found to be significant in the identification of the experimental spectra.

Theoretical calculations of transition energies and lifetimes are not available over a wide  $Z$ -range. The experimental and the theoretical studies are important since such results could be used as possible diagnostic tools for the analysis of very high temperature plasmas. Such plasmas are encountered for example in CTR devices and from the interaction of high-power lasers with matter.

The nonrelativistic Hartree-Fock program (without the inclusion of configuration mixing) was used to obtain the initial-state wave functions, the total energy and the spin-orbit parameter. The final-state total energy was similarly calculated. The mixing coefficients and the energy eigenvalues were then obtained in the intermediate coupling scheme. The electric quadrupole transitions  $3d^9 4s \rightarrow 3d^{10}$  and the electric dipole transitions  $3d^9 4p \rightarrow 3d^{10}$  were considered as a function of atomic number.

The relativistic contributions to the total energies are given by the diagonal matrix elements of  $H_m$  and  $H_d$  for each orbital, where  $H_m$  and  $H_d$  are the "mass-velocity" and "Darwin" Hamiltonians respectively.<sup>4</sup> The Hartree-Fock-Slater program of Hermann and Skillman, as modified by Bhalla et al.,<sup>4</sup> was used to calculate the relativistic corrections,  $\Delta E_R$ , to the

x-ray transition energies. The x-ray transition energies,  $E(= HF + \Delta E_R)$ , were calculated.

The transition rates were computed using the oscillator strengths (obtained with the HF wave functions) and the eigen vectors for  $Z = 40, 50, 53, 60, 70$  and  $80$ .

- <sup>1</sup>Charlotte E. Moore, N.B.S. Circular 467, U. S. Govt. Prtg. Office, Washington, D.C. (1952); E. Alexander, M. Even-Zohar, B. S. Fraenkel and S. Goldsmith, J. Opt. Soc. Am. 61, 508 (1971); P. G. Burkhalter, D. J. Nagel, and R. R. Whitlock, Phys. Rev. A 9, 2231 (1974).
- <sup>2</sup>C. L. Cocke et al., Phys. Rev. A (submitted for publication) 1975.
- <sup>3</sup>C. Froese-Fischer, Comp. Phys. Comm. 4, 107 (1972); and 1, 151 (1969).
- <sup>4</sup>F. Hermann and S. Skillman, Atomic Structure Calculations (Prentice-Hall, Englewood Cliffs, N. J., 1963); C. P. Bhalla, N. O. Folland and M. A. Hein, Phys. Rev. A 8, 649 (1973).

(C. P. Bhalla, C. L. Cocke, and S. L. Varghese)

## 10. THEORETICAL ATOMIC CROSS SECTION CALCULATIONS

### 10.1 K-Shell Ionization in Multielectron Atoms by Electron Impact Using the Single-Particle Glauber Approximation.

Comparison of Glauber and Born calculations for the ionization of atomic hydrogen by electron impact with experiment<sup>1</sup> indicated that the Glauber calculation was in agreement with observations at projectile energies near and above the peak of the cross section while the simpler Born results are as much as a factor of two larger than experiment. In order to conveniently extend the Glauber theory to multielectron targets a single particle Glauber approximation was developed which reduces to the simpler, widely used Born approximation at high energies. The single particle Glauber results (labeled GME2 and GME3) were in good agreement with observed total ionization cross sections in helium near and above the peak of the cross section, as shown in Fig. 1, while the Born results (labeled Bell-Kingston) were as much as 50% too large. Further calculations for electron ionization of lithium, boron, and neon indicate that differences between single particle Glauber and Born K-shell ionization cross sections become small as the target Z increases. A simple mathematical explanation has been found.

<sup>1</sup>J. E. Golden and J. H. McGuire, Phys. Rev. Letters 32, 1218 (1974).

(J. H. McGuire)

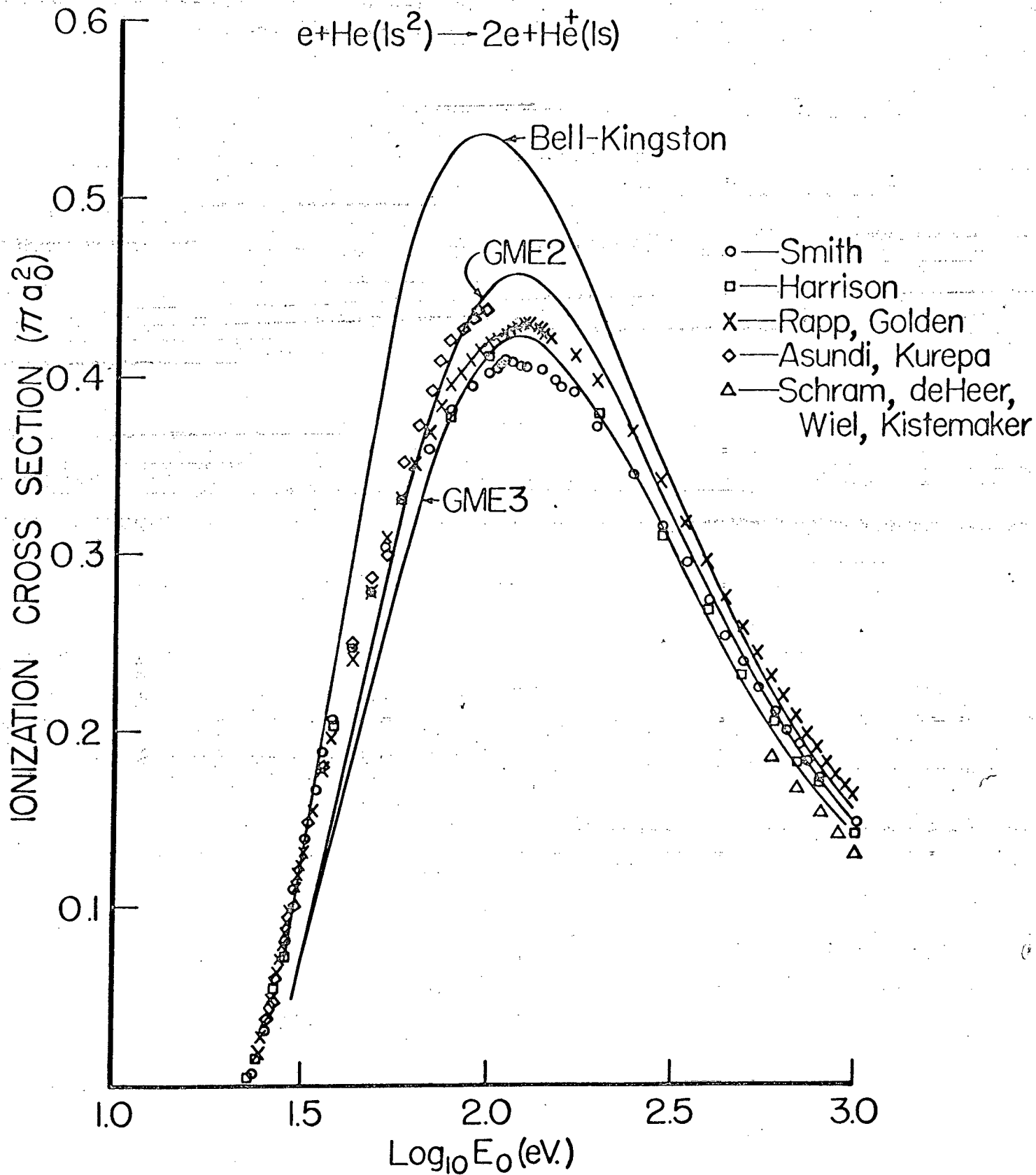


Fig. 1  
Sec. 10.1

## 10.2 K-Shell Ionization Cross Sections by Proton Impact Using the Single-Particle Glauber Approximation.

Despite good agreement between Glauber predictions and experiment for ionization of atomic hydrogen by electron impact, ionization predictions by proton impact lie beneath<sup>1</sup> observed results. In extending the single particle Glauber calculations to ionization of helium by proton impact, the Glauber results lie below the data while Born results were slightly above observations near the peak of the cross section. The most plausible, but not the only, explanation is that charge transfer to the continuum<sup>2</sup> contributes to the observed results. As  $Z$  increases, the differences between single particle Glauber and Born K-shell ionization cross sections decreases as shown in Fig. 1. For  $Z > 5$ , relatively large uncertainties arise due to uncertainties in the multielectron wave functions, especially the continuum wave functions. Thus the discrepancy between predictions and observations in neon taken by Richard *et al.* and in argon taken by Macdonald *et al.* may be due to inaccuracies of static rather than scattering wave functions.

<sup>1</sup>J. E. Golden and J. H. McGuire, Phys. Rev. A 12, 80 (1975).

<sup>2</sup>J. Macek, Phys. Rev. A 1, 235 (1970).  $\theta$

(J. E. Golden and J. H. McGuire)

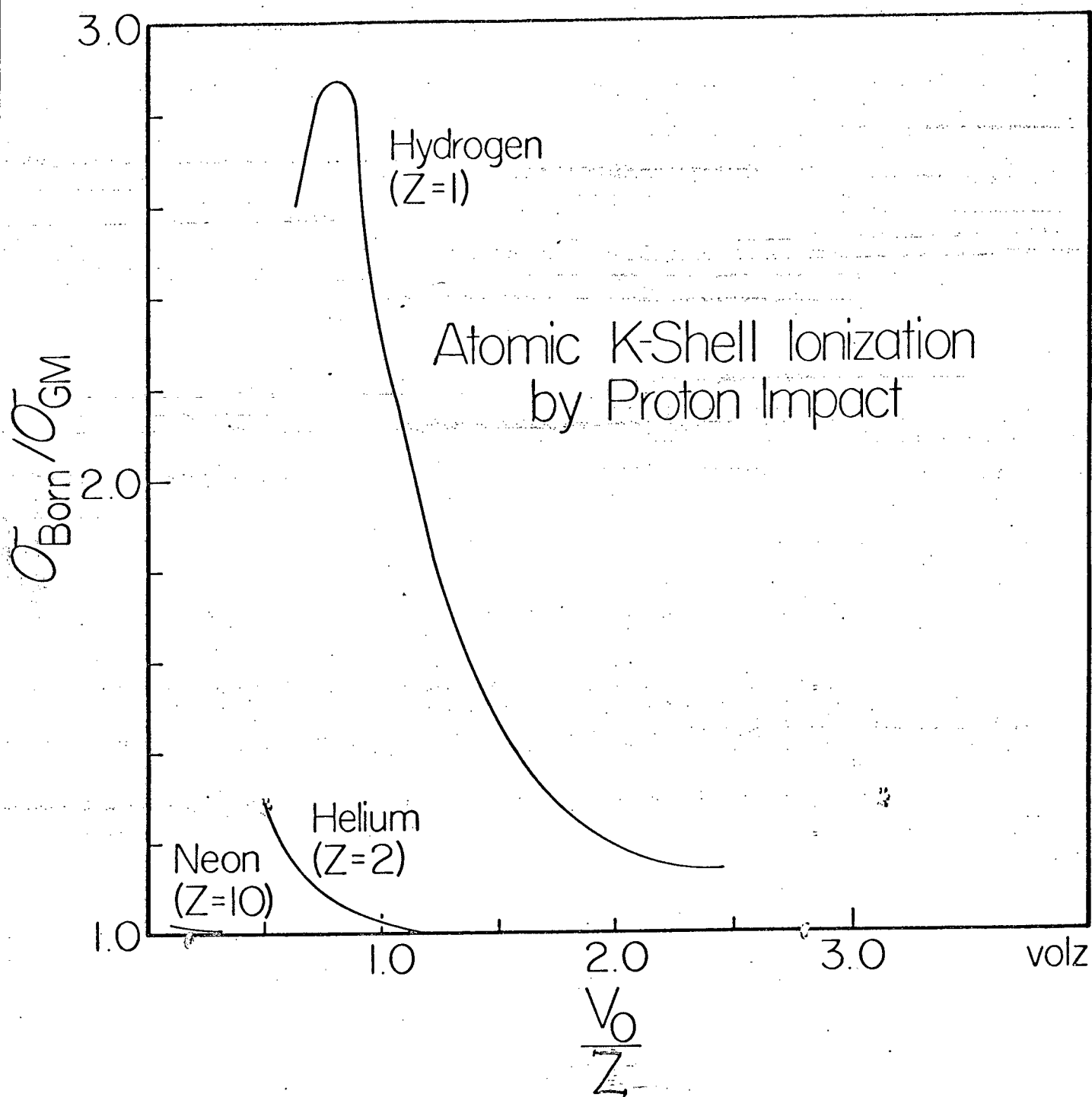


Fig. 1  
Sec. 10.2

### 10.3 Projectile Charge Dependence of Total Ionization Cross Sections in Atomic Hydrogen by Proton and Alpha Particle Impact.

Observed deviations from the projectile  $Z_1^2$  charge dependence predicted by the Born approximation may be due to a combination of factors. If the projectile charge is sufficiently large, unitarity may provide a constraint on the  $Z_1$  dependence. Since the Glauber approximation is approximately unitary, while Born is not, the effect of unitarity may become evident in the projectile charge dependence. Computing ionization cross sections in atomic hydrogen by alpha particle impact and using previous results for proton impact, we have plotted  $\sigma(Z_1)/Z_1^2\sigma(1)$  for  $Z_1 = 2$  as a function of energy shown in Fig. 1. The results suggest that in some regions the Glauber charge dependence differs significantly from that predicted by the Born approximation.

(J. E. Golden and J. H. McGuire)

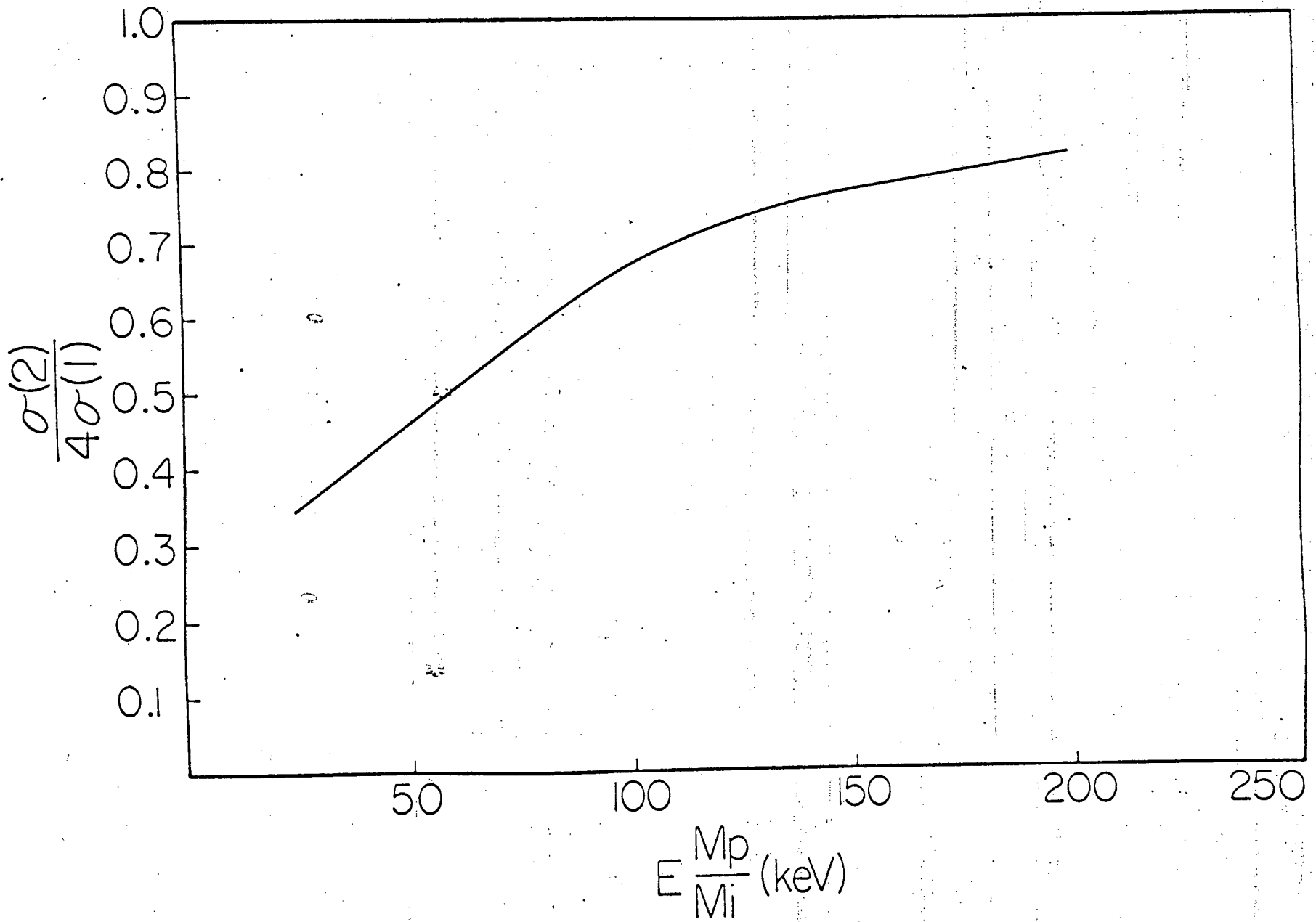


Fig. 1

Sec. 10.3

#### 10.4 Spectral Energy Distributions of Ejected Atomic Electrons.

While the shapes of the differential cross section,  $d\sigma/dk$ , predicted by the Glauber and Born calculations for the ionization of hydrogen are similar, the normalizations differ. Recent observations<sup>1</sup> for ionization of hydrogen by proton impact differ in shape as well as magnitude, with both predictions, although the Born results tend to be above the data while the Glauber results fall below. Subtracting the Glauber results from the data<sup>1</sup> leads to a distribution which peaks when the velocity of the ejected electron roughly matches the velocity of the projectile. This result supports the suggestion that charge transfer to the continuum may be an important scattering mechanism in some regions.

<sup>1</sup>J. Park, private communication.

(J. H. McGuire)

#### 10.5 Momentum Transfer Differential Cross Sections for Ionization.

As in atomic excitation, there are very large (i.e. orders of magnitude) differences between Glauber and Born predictions for the momentum transfer differential cross section,  $d\sigma/dq$ . We have computed double differential cross sections  $d^2\sigma/dk dq$  for K-shell ionization in a variety of targets by both electron and proton impact in the single particle Glauber and Born approximations. Since the calculations are done at a large number

of values of  $k$ , the differential cross section  $d\sigma/dq$  may be extracted.

(J. H. McGuire)

#### 10.6 Theoretical Definition of the Binomial Distribution of Single Electron Ionization and Excitation Probabilities.

Vacancy production in multielectron targets produced by the impact of heavy charged particles has been observed under a variety of conditions, some of which include multiple excitation and ionization. Most calculations of absolute cross sections pertain to vacancy production in an effective single electron system and do not explicitly detail the effects of multiple ionization and excitation. We assume that the total wave function of a multielectron target and colliding charged particle may be written as a product Hartree or uncorrelated Hartree-Fock wave function, and that the kinetic energy of the projectile is a c-number. The resulting total wave function may then be expressed as a product of single electron wave functions each of which evolves independently in time. It then follows that the probability amplitude factorizes and simple counting using unitarity results in a binomial distribution of single electron probabilities. Agreement of this approach with observed multiple ionization data has been established in some regions. Furthermore, this approach may be used to correlate some observations of the impact parameter dependence of ionization cross sections to multiple ionization observations. Our present interest, however, is to define the binomial distribution of probabilities

and to seek its limitations. It is not yet clear whether such an approach can be applied to charge transfer, or to multiple ionization of outer shell electrons by electron impact, or how this approach correlates to multiple scattering terms contained in the Glauber approximation.

(J. H. McGuire and L. Weaver)

#### 10.7 Application of a Charge Paired Born Approximation to Charge Transfer.

Over the past few years, a computer code has been developed to compute charge transfer cross sections using versions of the first Born approximation including various amounts of the internuclear interaction. It was found<sup>1</sup> that decent agreement with experiment could be obtained by using just enough of the internuclear interaction to match asymptotic boundary conditions. Calculations using this code were recently developed to investigate the angular distribution of the charge transfer cross sections from the K-shell of argon by proton impact. These calculations may be compared to recent observations by Cocke et al. A minimum predicted by the charge paired calculation, but absent in the simpler Brinkman-Kramers calculation, was not observed. On the other hand, the cross section at the larger angles is better represented by the charge paired Born calculation than by the Brinkman-Kramers prediction, which falls off too rapidly.

Some preliminary calculations were also done using Brinkman-Kramers and charge paired Born for charge capture from helium into various excited

states of <sup>+9</sup>F. These preliminary results suggest that the two theories predict different cross sections for capture into various levels. More definitive (and expensive) charge paired Born calculations are being deferred pending study of various general aspects of the charge transfer problem.

<sup>1</sup>K. Omidvar, J. E. Golden, J. H. McGuire, and L. Weaver, to be published.

(J. H. McGuire)

#### 10.8 Development of a Modified Eikonal Approximation for Charge Transfer.

An eikonal approximation for charge transfer has at least two advantages over Born approximations. First, it includes contributions from higher Born terms, which can be dominant at least in the very high energy limit. Furthermore, an eikonal approach includes the relative phase of the wave functions. This phase can depend on the internuclear separation, so that in charge transfer, unlike excitation and ionization, it can play<sup>1</sup> an important role. Both of these effects may contribute to total cross sections as well as angular distributions. Golden and McGuire have developed some phase terms in a Glauber-like development. The differential cross section for  $1s-1s$  transitions may be expressed as a one dimension integral, and if the internuclear term is dropped, a closed form expression results which reduces to the Brinkman-Kramers approximation as the phase contribution becomes small. Preliminary results for  $1s-1s$

charge capture in protons on atomic hydrogen are encouraging. A similar calculation of  $1s-1s$  capture for protons on argon can be generated with an effective one-electron picture.

<sup>1</sup>J. Macek, private communication.

(J. H. McGuire)

#### 10.9 DWBA Calculation of Excitation in Atoms and Ions by Charge Particles

Cross sections for the excitation and ionization of atoms by charged particles are more easily observed than cross sections for the excitation and ionization of ions by charged particles. Unfortunately, a rigorous calculation of cross sections ion-charged particle scattering is presently lacking, except, of course, for scattering of two-charged particles. An extension of the Born approximation to include long-ranged Coulomb interactions in the wave functions has been developed by Geltman,<sup>1</sup> among others. In this DWBA approximation Golden, Junker and McGuire have developed a mathematical technique, based on the use of prolate spheroidal coordinates, to compute excitation cross sections. As a Master's thesis project, Paul Simony has begun to examine, program, and test this technique for excitation in atoms and ions whose wave functions may be approximated by hydrogenic wave functions.

<sup>1</sup>S. Geltman, J. Phys. B 4, 1288 (1971).

(J. H. McGuire)

#### 10.10 SCA Predictions of 2s-2p Transition Probabilities by Direct Coulomb Excitation.

In some scattering processes, such as vacancy production in hydrogen by the impact of chlorine ions recently observed by Macdonald et al., it is evident that multi-step processes may be important. Furthermore, the transition of an electron from 2s-2p can alter the fluorescence yield and thus the analysis of such observations. A calculation has been undertaken for the 2s-2p transition probability as a function of impact parameter, 2s-2p energy splitting, projectile energy, projectile charge and target charge using the semiclassical Coulomb approximation (SCA). An estimate for 2s-2p excitation in hydrogen by chlorine impact at  $\sim 6$  MeV/amu supports the conjecture that such excitation occurs with large probability.

(J. H. McGuire)

#### 10.11 Development of Born Code Including Coulomb Deflection and Binding Energy Corrections.

There have been experimental tests of the theory<sup>1</sup> of binding energy and Coulomb deflection corrections to standard Born calculations of atomic ionization by charged particle impact carried out by Gray et al. Some of these observations test the theory in regions where tabulated Born results are unavailable. A Born code with options to include or exclude

either binding energy or Coulomb deflection corrections has been developed to support the analysis of experimental observations.

<sup>1</sup>G. Basbas, W. Brandt and R. Laubert, Phys. Rev. A 7, 983 (1973).

(J. H. McGuire)

#### 10.12 Role of Outer Shells in Born Cross Sections for K-Shell Ionization by Charged Particles.

Many standard applications of the Born approximation to K-shell vacancy production apply first order perturbation theory to the interaction between a projectile and an atomic target represented by a product wave function. We have shown that these standard Born predictions need not be restricted to one-electron ionization, but should be compared to experimental observations summed over all states corresponding to single K-vacancy production to include multiple vacancy production in other shells. These results are applicable to all targets in which the K shell is weakly perturbed even though the other shells may be strongly perturbed.

(J. H. McGuire and J. R. Macdonald)

## 11. SEARCH FOR HEAVY-ION RESONANCES

An investigation was made of the  $^{13}\text{C} + ^{16}\text{O}$  system. The primary aim of this investigation was to determine if there are resonances in this system that are similar to those found<sup>1</sup> in the  $^{12}\text{C} + ^{12}\text{C}$  system. Two exit channels were investigated: elastic scattering and gamma rays from two different daughter nuclei. Despite the presence of a slight anomaly in the elastic channels no evidence for correlated structure was discovered.

Thus the conclusion is made that no such structure exists in this system.

Preliminary data for the scattering of  $^{15}\text{N}$  from  $^{12}\text{C}$  has been obtained in the form of elastic scattering and alpha-reaction excitation curves. These data indicate structure similar to that observed<sup>2</sup> in the scattering of  $^{13}\text{C}$  from  $^{12}\text{C}$ .

<sup>1</sup>E. Almqvist, D. A. Bromley, and J. A. Kuehner, Phys. Rev. Lett. 4, 515 (1960); E. Almqvist, D. A. Bromley, J. A. Kuehner, and B. Whalen, Phys. Rev. 130, 1140 (1963).

<sup>2</sup>D. J. Crozier and J. C. Legg, Phys. Rev. Lett. 33, 782 (1974).

(J. C. Legg, R. Phillips, D. J. Crozier, and E. Dreyer)

## 12. LIFETIMES OF LOW-ENERGY STATES IN $^{21}\text{Ne}$

Lifetimes of states up to 6-MeV excitation in  $^{21}\text{Ne}$  have been measured by Doppler-shift attenuation in the  $^{12}\text{C}(^{13}\text{C},\alpha)^{21}\text{Ne}$  reaction at 17.4 MeV bombarding energy. An  $\alpha$ - $\gamma$  coincidence is used to make the measurements. The lifetimes obtained are not sensitive to nuclear stopping, and are smaller than previously accepted values. The data gives support to a Nilsson model description for the low-lying levels of  $^{21}\text{Ne}$ .

(G. G. Seaman, D. J. Crozier, J. C. Legg, and K. C. Shane)

### 13. NUCLEAR SCATTERING AND REACTIONS

#### 13.1 Analog Resonances and Possible $T_>$ Mixing in $^{77}\text{Br}$

The locations and widths of several analog resonances in  $^{77}\text{Br}$  have been measured by  $^{76}\text{Se}(p,p)$  and  $^{76}\text{Se}(p,p')$  excitation functions between proton bombarding energies of 3.1 and 4.5 MeV. Comparison of resonance spectroscopic factors to stripping spectroscopic factors show poor agreement, but spectroscopic factor ratios for states of the same spin and parity show good agreement except for the s-wave resonances. It is suggested that this disagreement may be explained by a mechanism of  $T_>$  mixing between  $\frac{1}{2}^+$  resonances.

(J. W. Gray and J. C. Legg)

#### 13.2 Systematics of Backward-Angle Elastic Alpha Scattering

Backward angle ( $\theta > 90^\circ$ ) cross sections for elastic alpha scattering from target nuclei  $32 \lesssim A \lesssim 100$  in the bombarding energy range  $15 \lesssim E \lesssim 40$  MeV, have been systematically investigated using all available data. A simple quantitative prescription for estimating the degree of backward enhancement  $\epsilon$  has been given, and shown to be strongly correlated with  $(\alpha,n)$  and  $(\alpha,\alpha')$  Q values and with compound-nucleus level densities. This correlation is described in terms of flux removal from high angular momentum ( $\ell$ ) entrance channels via  $\ell$ -dependent absorption potentials and compound-elastic scattering.

(J. S. Eck, W. J. Thompson, K. A. Eberhard, J. Schiele and W. Trombik)

### 13.3 Optical-Model Analysis of N+C and C+C Elastic Scattering

Additional data and optical model calculations for  $^{14}\text{N} + ^{12}\text{C}$  elastic scattering which expand and fortify the recent published optical model analysis of N + C and C + C elastic scattering by Delic<sup>1</sup> have been obtained. We have recently measured and analyzed elastic scattering excitation functions of  $^{14}\text{N} + ^{12}\text{C}$  at six center-of-mass angles between 55° and 120° at  $^{14}\text{N}$  bombarding energies between 15.0 and 25.0 MeV (corresponding to 6.92 through 11.5 MeV in the center-of-mass). Four angular distributions were measured at center-of-mass energies 6.92, 9.23, 9.92, and 10.85 MeV in the angular range from  $\theta_{\text{CM}} = 20^\circ$  to 135°. The main emphases in our work were threefold:

- 1) Search for any non-statistical structures in the excitation functions,
- 2) Study the compound contributions to the elastic scattering cross sections,
- 3) Perform a detailed optical model analysis for comparison with the results of the (pn) elastic transfer process reported by Von Oertzen<sup>2</sup> for  $^{14}\text{N} + ^{12}\text{C}$  elastic scattering and the results of the  $\ell$ -dependent optical model calculation reported by Robson.<sup>3</sup>

<sup>1</sup>G. Delic, Phys. Rev. Letters 34, 1468 (1975).

<sup>2</sup>W. von Oertzen, Proceedings of the Symposium on Heavy-Ion Scattering, ANL (1971) edited by Siemssen.

<sup>3</sup>D. Robson, *ibid.*

(J. S. Eck, J. H. Johnson, D. O. Elliott, and W. J. Thompson)

#### 13.4 Comparison of One and Two-Neutron Transfer near the Coulomb Barrier for the $^{27}\text{Al}(^{18}\text{O}, ^{16}\text{O})^{29}\text{Al}$ , $^{27}\text{Al}(^{18}\text{O}, ^{17}\text{O})^{28}\text{Al}$ and $^{27}\text{Al}(^{13}\text{C}, ^{12}\text{C})^{28}\text{Al}$ Reactions

Total reaction cross sections for the transfer reactions  $^{27}\text{Al}(^{18}\text{O}, ^{16}\text{O})^{29}\text{Al}$ ,  $^{27}\text{Al}(^{18}\text{O}, ^{17}\text{O})^{28}\text{Al}$  and  $^{27}\text{Al}(^{13}\text{C}, ^{12}\text{C})^{28}\text{Al}$  are measured for center-of-mass energies between 13 and 20 MeV for  $^{18}\text{O}$  projectiles and between 11 and 17.5 MeV for  $^{13}\text{C}$  projectiles. The reaction products,  $^{29}\text{Al}$  and  $^{28}\text{Al}$ , beta decay to  $^{29}\text{Si}$  and  $^{28}\text{Si}$ , respectively, and the subsequent  $\gamma$  decays of  $^{29}\text{Si}$  and  $^{28}\text{Si}$  are measured. Due to the relatively long beta decay half lives, data were taken in a beam-off mode, resulting in very clean spectra. Total cross sections were calculated and compared with a theoretical model for barrier penetration proposed by C. Y. Wong. Differences between  $^{18}\text{O}$  induced one and two-neutron total transfer reaction cross sections are discussed.

(S. A. Schiller and J. S. Eck)

#### 13.5 The Proton Optical-Model Potential Near the Coulomb Barrier

Proton elastic scattering data from  $^{197}\text{Au}$ ,  $^{208}\text{Pb}$  and  $^{209}\text{Bi}$  at energies near the Coulomb barrier are analyzed. The energy dependences of the real volume and imaginary surface-derivative potential depths  $V_R$  and  $W_{SF}$  of a local optical-model potential with fixed geometric parameters are found to be much more rapid than at higher energies. The strong

energy dependence of  $V_R$  near the Coulomb barrier is explained in terms of the non-locality of the nucleon-nucleus interaction.

(J. S. Eck and W. J. Thompson)

### 13.6 Total Cross Sections for the $^{19}\text{F}(^{13}\text{C}, ^{12}\text{C})^{20}\text{F}$ and $^{23}\text{Na}(^{13}\text{C}, ^{12}\text{C})^{24}\text{Na}$ Reactions

Total cross sections for the  $(^{13}\text{C}, ^{12}\text{C})$  reaction on  $^{19}\text{F}$  at laboratory energies of 9.0 to 25.0 MeV and on  $^{23}\text{Na}$  at energies of 10.5 to 19.5 MeV were measured by detecting the gamma rays from excited states and from the decay of the radioactive ground states. At energies well below the Coulomb barrier the cross sections are compared with a semi-classical distorted wave Born approximation calculation, and spectroscopic factors are extracted.

(H. Laumer and G. G. Seaman)

### 13.7 Energy Loss of Low-Energy $^{40}\text{Ca}$ Ions in Carbon

The energy loss of  $^{40}\text{Ca}$  in carbon at less than 335 keV energy has been measured by detecting the energy of Doppler-shifted gamma rays from recoiling Ca ions. The energy loss mechanism can be suitably described as 1.15 and 0.7 times the theoretical values for electronic and

nuclear stopping.

(K. C. Shane, H. Laumer, and G. G. Seaman)

## 14. TRACE ELEMENT ANALYSIS

### 14.1 The Determination by X-Ray Observation of Bromine and Zinc Levels in Untreated Wheat Flour

The recently developed method of trace element analysis by observation of characteristic x-rays with a lithium-drifted silicon detector was used to study levels of heavy elements in wheat flour.

A 4 MeV proton beam bombarded on the samples was used to produce the x rays. The various samples obtained from a pilot mill were each found to contain quantities of zinc at levels of about 2 to 54 parts per million and bromine at levels of 2 to 14 parts per million. An attempt is made to correlate these zinc and bromine concentrations to the standard analyses of ash content and protein level used for flour.

(R. A. Martin, G. G. Seaman, and Arlin Ward)

### 14.2 Trace-Element Analysis by X-ray Fluorescence with an External Proton Beam

Trace elements in samples of wheat flour have been studied by proton-induced x-ray fluorescence as discussed in the previous section. Samples were wafers about one mm thick, prepared by mixing a few drops of distilled water with the flour to form a paste, which was then allowed to dry in air. Under proton bombardment in a vacuum system, a substantial amount of moisture was driven off, thus adversely affecting the vacuum.

Although suitable drying procedures were found, an alternative procedure was sought that would require less preparation. This led to a study of trace elements in samples in air by use of an external proton beam.

The experiment successfully showed that an external proton beam provides an alternate method for studying wet samples to determine the composition of trace elements. The method may prove especially convenient for certain samples prepared from liquids, such as blood. Sample changing and sample preparation are much more easily handled than for samples placed in a vacuum system. Also, samples will cool more readily than in a vacuum, thus reducing heating problems. Further experiments with exit foils may yield a better choice than mylar or Ni, but these two have been shown to be acceptable at the low currents needed.

(G. G. Seaman and K. C. Shane)

## 15. ATOMIC AND NUCLEAR PHYSICS LABORATORY PERSONNEL

### Faculty

C. P. Bhalla, Professor  
C. L. Cocke, Associate Professor  
J. S. Eck, Associate Professor  
T. J. Gray, Visiting Professor<sup>1</sup>  
J. C. Legg, Professor  
J. R. Macdonald, Professor  
J. H. McGuire, Assistant Professor  
E. H. Pedersen, Visiting Assistant Professor<sup>2</sup>  
P. Richard, Professor  
E. Salzbom, Visiting Professor<sup>3</sup>  
G. G. Seaman, Associate Professor  
N. Stolterfoht, Visiting Professor<sup>4</sup>

### Research Staff

Mohammed Ahmed, Research Associate  
D. Crozier, Research Associate<sup>5</sup>  
S. Czuchlewski, Research Associate<sup>6</sup>

### Laboratory Staff

E. Feldl, Design Engineer  
G. Geelan, Draftsman  
K. Jamison, 3 MV Accelerator Supervisor  
R. Krause, Accelerator Engineer  
D. Richard, Secretary  
M. Ross, Electronics Engineer<sup>7</sup>  
J. Tormey, Machine Shop Foreman<sup>7</sup>  
M. Wells, Accelerator Technician

### Undergraduate Research Assistants

Steve Howe  
Jim Oltjen<sup>8</sup>  
John Shellenberger

Graduate Research Assistants

Clarence Annett<sup>9</sup>  
Eric Dreyer  
Jack E. Golden<sup>10</sup>  
James A. Guffey  
James M. Hall  
Keith A. Jamison<sup>11</sup>  
Robert L. Kauffman<sup>12</sup>  
Robert Phillips  
Russell Randall<sup>13</sup>  
Paul Simony  
James N. Wickberg  
Clifford W. Woods<sup>14</sup>

---

<sup>1</sup>On leave from North Texas State University, Denton, Texas.

<sup>2</sup>On leave from University of Aarhus, Aarhus, Denmark for 12 months.

<sup>3</sup>On leave from University of Giessen, Giessen, West Germany for 12 months.

<sup>4</sup>On leave from Hahn-Meitner Institute, Berlin, West Germany for 1 month.

<sup>5</sup>Terminated appointment August 31, 1975.

<sup>6</sup>Present address: Los Alamos Scientific Laboratory.

<sup>7</sup>Supported by Kansas State University.

<sup>8</sup>Present address: University of Giessen, Giessen, West Germany.

<sup>9</sup>Terminated August 31, 1975 following three-month appointment.

<sup>10</sup>Present Address: Fusion Energy Corporation, Princeton, New Jersey.

<sup>11</sup>3 MV accelerator supervisor.

<sup>12</sup>Present Address: Bell Laboratories, Murray Hill, New Jersey.

<sup>13</sup>Present Address: Dresser Industries, Houston, Texas.

<sup>14</sup>Present Address: Los Alamos Scientific Laboratory, Los Alamos, New Mexico.

16. ADVANCED DEGREES AWARDED DURING 1974-75 ACADEMIC YEAR

- Jack E. Golden, Ph.D. "Calculation of Total Cross Sections for the Ionization of Atomic Systems by Charged Particle Impact Using the Glauber Approximation"
- James A. Guffey, M.S. "A Comparison Between Experimental Electron Capture Data and a Modified Brinkman-Kramers Calculation"
- Keith A. Jamison, M.S. "Study of  $K\alpha$  X Rays from Al, Sc, and Ti Following Bromine-Ion Bombardment"
- R. L. Kauffman, Ph.D. "High Resolution Study of the Charge State Dependence of Ion-Induced X Rays"
- Russell Randall, Ph.D. "Impact Parameter Dependence for Inner-Shell Vacancy Production for Fast Ion-Atom Collisions"
- Loren M. Winters, Ph.D. "K X-ray Production by Chlorine and Sulfur Ions in Thin Gas Targets"
- C. W. Woods, Ph.D. "K-Shell Auger Electron Production Cross Sections from Ion Bombardment"

## 17.1 Published Papers Supported by ERDA Contract E(11-1)-2130

1. "K X-Ray Emission from 20- to 36-MeV Fluorine Projectiles Following Electron Capture to Excited States,"  
M. D. Brown, L. D. Ellsworth, J. A. Guffey, T. Chiao, E. W. Pettus, L. M. Winters, and J. R. Macdonald, Phys. Rev. A 10, 1255-1262 (1974).
2. "Analog Resonances and Possible  $T_{\gamma}$  Mixing in  $^{77}\text{Br}$ ,"  
J. W. Gray and J. C. Legg, Phys. Rev. C 10, 2577-2583 (1974).
3. "Direct Extraction of a  $^{12}\text{C}^{-}$  Beam from a Diode Ion Source,"  
J. S. Eck and D. O. Elliott, Nucl. Inst. and Meth. 121, 411-412 (1974).
4. "Total Cross Sections for the  $^{19}\text{F}$ ( $^{13}\text{C}$ ,  $^{12}\text{C}$ ) $^{20}\text{F}$  and  $^{23}\text{Na}$ ( $^{13}\text{C}$ ,  $^{12}\text{C}$ ) $^{24}\text{Na}$  Reactions,"  
H. Laumer and G. G. Seaman, Phys. Rev. C 10, 2159-2165 (1974).
5. "Ne K Auger Cross Sections from 1.5 MeV/amu H, O and F,"  
C. W. Woods, R. L. Kauffman, K. A. Jamison, C. L. Cocke, and Patrick Richard, J. Phys. B: Atom. and Molec. Phys. Letters 7, L474-77 (1974).
6. "Multiplet Effects in High Resolution Ne  $K\alpha$  Structure"  
R. L. Kauffman, C. W. Woods, K. A. Jamison, and P. Richard, Phys. Letters 50A, 117-119 (1974).
7. "Charge-State Dependence of the Ne K Fluorescence Yield Deduced from High Resolution Emission Spectra,"  
N. Stolterfoht, D. Schneider, P. Richard and R. L. Kauffman, Phys. Rev. Letters 33, 1418-1422 (1974).
8. "Neon  $K\alpha$ ,  $K\beta$  Satellite Structure Induced by 80-MeV Argon-Ion Impact,"  
J. R. Mowat, R. Laubert, I. A. Sellin, R. L. Kauffman, M. D. Brown, J. R. Macdonald and P. Richard, Phys. Rev. A 10, 1446-1449 (1974).
9. "K X-Ray Production in Single Collisions of Chlorine and Sulphur Ions"  
L. Winters, M. D. Brown, L. D. Ellsworth, T. Chiao, E. W. Pettus and J. R. Macdonald, Phys. Rev. A 11, 174-187 (1975).
10. "The Determination by X-Ray Observation of Bromine and Zinc Levels in Untreated Wheat Flour,"  
R. A. Martin, G. G. Seaman, and A. Ward, Cereal Chemistry 52, 138-144 (1975).
11. " $K\alpha$  Satellite X Rays in Al, Sc, and Ti Following Bromine-Ion Bombardment,"  
K. A. Jamison, C. W. Woods, R. L. Kauffman and Patrick Richard, Phys. Rev. A 11, 505-508 (1975).

12. "The Proton Optical-Model Potential Near the Coulomb Barrier,"  
J. S. Eck and W. J. Thompson, Nucl. Phys. A 237, 83-92 (1975).
13. "Argon and Krypton X-Ray Production by Fluorine Projectiles of Different Charge States,"  
S. J. Czuchlewski, J. R. Macdonald and L. D. Ellsworth, Phys. Rev. A 11, 1108-1113 (1975).
14. "Relative Multiple Ionization Cross Sections of Neon by Projectiles in the 1-2 MeV/amu Energy Range,"  
R. L. Kauffman, C. W. Woods, K. A. Jamison, and Patrick Richard, Phys. Rev. A 11, 872-83 (1975).
15. "Back Angle Anomalies in Alpha Scattering: Inelastic Scattering from the Calcium Isotopes,"  
W. Trombik, K. A. Eberhard, and J. S. Eck, Phys. Rev. C 11, 685-92 (1975).
16. "Lifetimes of the  $2^3S_1$  State in Heliumlike Sulphur and Chlorine,"  
J. A. Bednar, C. L. Cocke, B. Curnutte and R. Randall, Phys. Rev. A 11, 460-464 (1975).
17. "Anisotropy of Characteristic K-Shell X Rays from Heavy-Ion-Atom Collisions,"  
E. Horsdal Pedersen, S. J. Czuchlewski, M. D. Brown, L. D. Ellsworth, and James R. Macdonald, Phys. Rev. A 11, 1267-70 (1975).
18. "Ne K-Shell Vacancy Production by Intermediate Energy F Ions,"  
C. W. Woods, R. L. Kauffman, K. A. Jamison, N. Stolterfoht, and Patrick Richard, J. Phys. B: Atom. and Molec. Phys. Letters 8, L61-64 (1975).
19. "Polarization Fractions of K X Rays Emitted by Fast Fluorine Ions Incident in Different Charge States on Helium,"  
S. J. Czuchlewski, L. D. Ellsworth, J. A. Guffey, E. H. Pedersen, E. Salzbom, and J. R. Macdonald, Phys. Letters 51A, 309-11 (1975).
20. "Trace Element Analysis by X-Ray Fluorescence with an External Proton Beam,"  
G. G. Seaman and K. C. Shane, Nucl. Inst. & Meth. 126, 473-74 (1975).
21. "Optical-Model and Coupled-Channels Calculations in Quantum Mechanical Scattering,"  
S. D. Doyle, J. S. Eck, W. J. Thompson and O. L. Weaver, Am. Jour. of Phys. 43, 677-82 (1975).
22. "Impact Parameter Dependence of Inner-Shell Ionization Probabilities,"  
C. L. Cocke, Use of Small Accelerators in Research and Teaching, Vol. 1, 427-35 (1974), Conf-741040-P2.
23. "An Integral Representation for the Glauber Scattering Amplitude for Direct Coulomb Ionization by Charged Particles,"  
J. E. Golden and J. H. McGuire, Phys. Rev. A 12, 80-84 (1975).

24. "Role of Outer Shells in Born Cross Sections for K-Shell Ionization by Charged Particles,"  
J. H. McGuire and J. R. Macdonald, Phys. Rev. A 11, 146-48 (1975).
25. "Argon K-Auger Cross Sections in Collisions with 30-MeV Fluorine Ions,"  
C. L. Cocke, R. R. Randall and B. Curnutte, IX ICPEAC Abstracts Vol. 2,  
933-34 (1975), edited by R. Geballe and J. S. Risley.
26. "Comparisons of Cross Sections and  $\bar{\omega}_K$  in 40-50 MeV  $Cl^{+q}+Ne$ ,"  
R. L. Kauffman, C. W. Woods, K. A. Jamison, and P. Richard, IX ICPEAC  
Abstracts Vol. 2, 939-46 (1975), edited by R. Geballe and J. S. Risley.
27. "Auger Electrons from Double K-Shell Vacancy States in Ne,"  
C. W. Woods, R. L. Kauffman, K. A. Jamison, N. Stolterfoht, and P. Richard,  
IX ICPEAC Abstracts Vol. 1, 417-18 (1975), edited by R. Geballe and J. S. Risley.

17.2 Papers Submitted for Publication and Supported by ERDA Contract E(11-1)-2130.

1. "K-Shell Auger-Electron Hypersatellites of Ne,"  
C. W. Woods, R. L. Kauffman, K. A. Jamison, N. Stolterfoht, and Patrick Richard, accepted for publication in Oct. Phys. Rev. A.
2. "Experimental Impact-Parameter Dependent Probabilities for K-Shell Vacancy Production by Fast Heavy-Ion Projectiles,"  
R. R. Randall, J. A. Bednar, B. Curnutte and C. L. Cocke, submitted to Phys. Rev. A.
3. "Energy Loss of Low-Energy  $^{40}\text{Ca}$  Ions in Carbon,"  
K. C. Shane, H. Laumer and G. G. Seaman, submitted to J. App. Phys.
4. "Systematics of Backward-Angle Elastic Alpha Scattering,"  
J. S. Eck, W. J. Thompson, K. A. Eberhard, J. Schiele and W. Trombik, accepted for publication in Nuclear Physics.
5. "Optical-Model Analysis of N+C and C+C Elastic Scattering,"  
J. S. Eck, J. H. Johnson, D. O. Elliott and W. J. Thompson, accepted for publication Physical Review Letters, Comments.
6. "Comparison of One- and Two-Neutron Transfer Near the Coulomb Barrier for the  $^{27}\text{Al}(^{18}\text{C}, ^{16}\text{C})^{29}\text{Al}$ ,  $^{27}\text{Al}(^{18}\text{O}, ^{17}\text{O})^{28}\text{Al}$  and  $^{27}\text{Al}(^{13}\text{C}, ^{12}\text{C})^{28}\text{Al}$  Reactions,"  
S. A. Schiller and J. S. Eck, accepted for publication in Zeitschrift für Physik.
7. "Single-Electron Born Approximation for Charge Transfer from Multi-electron Atoms to Protons,"  
K. Omidvar, J. E. Golden, J. H. McGuire and L. Weaver, submitted to Phys. Rev. A.
8. "Radiative Auger Effect in Ion-Atom Collisions,"  
P. Richard, K. A. Jamison, R. L. Kauffman, C. W. Woods, and J. H. Hall, to be published in August Physics Letters.
9. "Neon K Fluorescence Yields for  $\text{N}^{\text{Q}+}$ -Induced Collisions,"  
F. Hopkins, C. W. Woods, R. L. Kauffman, K. A. Jamison, and P. Richard, submitted to J. Phys. B.
10. "Lifetimes of Low-Energy States in  $^{21}\text{Ne}$ ,"  
G. G. Seaman, D. J. Crozier, J. C. Legg, and K. C. Shane, submitted to Nuclear Physics.

17.3 Papers Submitted for Publication and Supported by ERDA Contract  
E(11-1)-2753

1. "X Rays from Foil-Excited Iodine Beams,"  
C. L. Cocke, S. L. Varghese, J. A. Bednar, C. P. Bhalla, B. Curnutte,  
R. L. Kauffman, R. Randall, P. Richard, C. W. Woods, and J. H.  
Scofield, submitted to Phys. Rev. A.
2. "Radiative Electron Rearrangement: A Proposed Description for Low  
Energy Satellites in Ion-Atom Collisions,"  
K. A. Jamison, J. M. Hall and Patrick Richard, submitted to J. Phys.  
B: Atom. & Molec Phys. Letters.
3. "Relative Multiple Ionization Cross Sections of Neon,"  
C. P. Bhalla, submitted to J. Phys. B: Atom. & Molec Physics Letters.
4. "Lifetimes and Fluorescence Yields of Three-Electron Ions,"  
C. P. Bhalla and A. N. Gabriel, to be published in 1975 Beam-Foil  
Conference Proceedings, Gatlinburg,
5. "Relative Multiple Ionization Cross Sections of Neon by Oxygen Ions,"  
C. P. Bhalla, submitted to Physics Letters.
6. "Total Cross Sections for the Ionization of Atomic Hydrogen by  
Alpha Particle Impact Using the Glauber Approximation,"  
J. E. Golden and J. H. McGuire, submitted to J. Phys. B: Atom. &  
Molec. Physics Letters.
7. "Glauber Cross Sections for Inner-Shell Ionization in Multielectron  
Targets by Electron Impact,"  
J. E. Golden and J. H. McGuire, submitted to Phys. Rev. A.
8. "Enhancement of Radiative Electron Rearrangement in Si by He<sup>+</sup>  
Bombardment,"  
J. Oltjen, R. L. Kauffman, C. W. Woods, J. M. Hall, K. A. Jamison,  
and Patrick Richard, submitted to Physics Letters.
9. "Lifetime Measurement of the <sup>3</sup>P<sub>1</sub> State of Heliumlike Sulphur,"  
S. L. Varghese, C. L. Cocke, B. Curnutte, and R. R. Randall,  
to be published in 1975 Beam-Foil Conference Proceedings, Gatlin-  
burg.
10. "Relativistic Contributions to Transition Energies in NiI and CuI  
Isoelectronic Sequences,"  
C. P. Bhalla, C. L. Cocke, and S. L. Varghese, to be published in  
1975 Beam-Foil Conference Proceedings, Gatlinburg.
11. "Relative Multiple Ionization Cross Sections of Neon by Projectiles  
in the 1-2 MeV/amu Energy Range,"  
C. P. Bhalla, to be published in 1975 Beam-Foil Conference  
Proceedings, Gatlinburg.

#### 17.4 Abstracts of Contributed Papers

1. "Systematics of Backward-Angle Elastic Alpha Scattering,"  
J. S. Eck and W. J. Thompson, BAPS 19, 1013 (1974).
2. "Additional Resonances in  $^{12}\text{C} + ^{13}\text{C}$ ,"  
J. C. Legg and D. J. Crozier, BAPS 19, 1012 (1974).
3. "Charge State Dependence of Ne K X Rays from 40 MeV Cl Bombardment,"  
Patrick Richard, R. L. Kauffman, K. A. Jamison, S. Czuchlewski,  
and C. W. Woods, BAPS 19, 1181 (1974).
4. "Charge State Dependence of Ne K Fluorescence Yields,"  
N. Stolterfoht, D. Schneider, P. Richard, R. L. Kauffman,  
BAPS 19, 1181 (1974).
5. "Multiple Ionization of Ne by Semi-Swift Light Heavy Ions,"  
Robert L. Kauffman, C. W. Woods, K. A. Jamison, and Patrick  
Richard, BAPS 19, 1185 (1974).
6. " $K\alpha$  Satellite X Rays in Al, Sc, and Ti Following Bromine-Ion  
Bombardment,"  
K. A. Jamison, C. W. Woods, Robert L. Kauffman, and Patrick Richard,  
BAPS 19, 1180 (1974).
7. "Projectile Charge Dependence of the Ne K-Shell Auger Electron  
Production Cross Section,"  
C. W. Woods, Robert L. Kauffman, K. A. Jamison, C. L. Cocke, and  
Patrick Richard, BAPS 19, 1185 (1974).
8. "Metastable X-Ray Emitters in Highly Ionized Iodine,"  
C. L. Cocke, P. Richard, J. A. Bednar, B. Curnutte, R. Kauffman,  
R. Randall and C. W. Woods, BAPS 19, 1181 (1974).
9. "Impact Parameter Dependence of Probability for Argon K-Shell  
Ionization by Fast C & F Ions,"  
R. Randall, C. L. Cocke, B. Curnutte, and J. A. Bednar,  
BAPS 19, 1180 (1974).
10. "Optical-Model and Coupled-Channels Calculations in Quantum Mechanics,"  
S. D. Doyle, J. S. Eck, W. J. Thompson, and O. L. Weaver, BAPS 20,  
101 (1975).
11. "A Comparison of Experimental Electron Capture Data to a Modified  
Brinkman-Kramers Calculation,"  
J. A. Guffey and J. R. Macdonald, BAPS 19, 1201 (1974).
12. "Angular Distributions and Polarization Fractions of Target X Rays  
from Heavy-Ion Atom Collisions,"  
S. J. Czuchlewski, E. H. Pedersen, M. D. Brown, L. D. Ellsworth,  
and J. R. Macdonald, BAPS 19, 1184 (1974).
13. "Angular Distributions and Polarization Fractions of Projectile X Rays  
from Heavy-Ion Atom Collisions,"  
E. H. Pedersen, S. J. Czuchlewski, M. D. Brown, L. D. Ellsworth,  
and J. R. Macdonald, BAPS 19, 1185 (1974).

14. " $^{12}\text{C} + ^{13}\text{C}$  Resonances,"  
D. J. Crozier and J. C. Legg, BAPS 20, 54 (1975).
15. "Projectile Size Effects in Quadrupole Deformation Measurements,"  
J. S. Eck, D. O. Elliott, and W. J. Thompson, BAPS 20, 56 (1975).
16. "Formation Cross Sections for Li-like and Hypersatellite Auger  
Electrons of Ne,"  
Patrick Richard, C. W. Woods, Robert L. Kauffman, K. A. Jamison,  
and N. Stolterfoht, BAPS 20, 675 (1975).
17. "Excitation Functions for the  $^{13}\text{C} + ^{16}\text{O}$  Systems,"  
J. C. Legg, R. L. Phillips, and D. J. Crozier, BAPS 20, 664 (1975).
18. "Chlorine K X-Ray Production Cross Sections for Cl Ions in  $\text{H}_2$  and  
He Gases"  
J. R. Macdonald and E. H. Pedersen, BAPS 20, 674 (1975).
19. "Systematic Study of Ar K X-Ray Production Cross Sections by  
Energetic Heavy Ions with  $Z_1 < 9$ ,"  
E. Salzborn, J. Guffey, L. D. Ellsworth, and J. R. Macdonald,  
BAPS 20, 639 (1975).

## 17.5 INVITED TALKS PRESENTED BY STAFF

"Impact Parameter Dependence of Inner-Shell Ionization Probabilities," C. L. Cocke - Use of Small Accelerators in Research and Teaching, Vol. 1, 427-35 (1974) Conf-741040-P1, Denton, Texas.

"Experimental Studies of Atomic Processes in Inner-Shells Using Highly Stripped Heavy Ions," J. R. Macdonald Annual Meeting of DEAP in Chicago, BAPS 19, 1189-90 (1974).

"Systematics of Backward-Angle Elastic and Inelastic Alpha Scattering," John S. Eck - APS Meeting Anaheim, BAPS 20, 95 (1975).

"High Energy Atomic Physics at Accelerators," C. L. Cocke Midwest Accelerator Conference, Madison, Wisconsin (1975).

"Inner Shell Studies with Bare Nuclei as Projectiles," J. R. Macdonald - Fourth International Seminar on Ion-Atom Collisions (ISIAC 1975, Stanford University, Stanford, Ca.)

"Single-Step/Multi-Step Processes in Ion-Atom Single Collisions," C. L. Cocke - Fourth International Seminar on Ion-Atom Collisions (ISIAC 1975, Stanford University, Stanford, Ca.)

"Experimental Studies of Target and Projectile X Radiation in High Velocity Atomic Collisions," J. R. Macdonald IX ICPEAC, Seattle (1975).

"X Rays from Foil-Excited Beams at Tandem Energies," C. L. Cocke Fourth International Conference on Beam-Foil Spectroscopy, Gatlinburg (1975).

"Atomic Physics Studies with Accelerated Heavy Ions," J. R. Macdonald - Annual Meeting of Kansas Academy of Science (1975, Kansas State University, Manhattan, Kansas)

## 17.6 Review Papers for Textbook Publication

"Ion-Atom Collisions" (Chapter II) for Atomic Inner-Shell Processes, edited by Bernd Crasemann (Academic Press, Inc., 1974)  
(Patrick Richard)

"X-Ray Region" (Chapter III) for Methods of Experimental Spectroscopy, edited by Dudley Williams (Academic Press, Inc., 1975)  
(Robert L. Kauffman and Patrick Richard)

"Beam-Foil Spectroscopy" (Chapter IV) for Methods of Experimental Spectroscopy, edited by Dudley Williams (Academic Press, Inc., 1975)  
(C. L. Cocke)

"Gamma-Ray Region" (Chapter III) for Methods of Experimental Spectroscopy, edited by Dudley Williams (Academic Press, Inc., 1975)  
(J. C. Legg and G. G. Seaman)

## 18. ACKNOWLEDGMENT OF SUPPORT

This report is prepared specifically for the Energy Research and Development Administration and is being submitted, as required, simultaneously with the renewal proposal for ERDA Contract E(11-1)-2130 entitled "Atomic and Nuclear Research With Accelerators."

Additional acknowledgments for partial support of the reported work are given to:

(1) ERDA Contract E(11-1)-2753 entitled "Fusion Related Atomic Physics,"

(2) USONR Contract 00014-75-C-0490 for partial support of C. L. Cocke and for the Auger electron cylindrical mirror analyzer,

(3) U. S. Army Research Office Contract DAHC04-74-G-0137 for partial support of C. P. Bhalla, and

(4) Robert A. Welch Foundation and Sponsored Research Fund, State of Texas, for partial support of T. J. Gray.